

2014-01-01

Design Optimization of the Heat Transfer Model for a High Heat Flux Test Facility

Linda Hyemin Yoon

University of Texas at El Paso, lhyoon@Miners.utep.edu

Follow this and additional works at: https://digitalcommons.utep.edu/open_etd



Part of the [Mechanical Engineering Commons](#)

Recommended Citation

Yoon, Linda Hyemin, "Design Optimization of the Heat Transfer Model for a High Heat Flux Test Facility" (2014). *Open Access Theses & Dissertations*. 1380.

https://digitalcommons.utep.edu/open_etd/1380

This is brought to you for free and open access by DigitalCommons@UTEP. It has been accepted for inclusion in Open Access Theses & Dissertations by an authorized administrator of DigitalCommons@UTEP. For more information, please contact lweber@utep.edu.

DESIGN OPTIMIZATION OF THE HEAT TRANSFER MODEL FOR A HIGH HEAT FLUX
TEST FACILITY

LINDA HYEMIN YOON
Department of Mechanical Engineering

APPROVED:

Ahsan Choudhuri , Ph.D., Chair

Norman Love Jr., Ph.D.

Cristian Botez, Ph.D.

Charles Ambler, Ph.D.

Dean of the Graduate School

Copyright ©

by

Linda Hyemin Yoon

2014

Dedication

This report is dedicated to my family and friends who have supported me through my life.

DESIGN OPTIMIZATION OF THE HEAT TRANSFER MODEL FOR A HIGH HEAT FLUX
TEST FACILITY

by

LINDA HYEMIN YOON, B.S. Mechanical Engineering

THESIS

Presented to the Faculty of the Graduate School of

The University of Texas at El Paso

in Partial Fulfillment

of the Requirements

for the Degree of

MASTER OF SCIENCE

Department of Mechanical Engineering

THE UNIVERSITY OF TEXAS AT EL PASO

December 2014

Acknowledgements

I would like to acknowledge the faculty and staff of the Mechanical Engineering department at the University of Texas at El Paso and my graduate advisor Dr. Ahsan Choudhuri from the University of Texas at El Paso. I would like to thank NASA Johnson Space Center (JSC) for the financial support and mentorship in this project. The material in this project is based upon work supported by NASA under award No(s) NNX09AV09A. I would also like to recognize my mentor Dr. John C. Melcher from NASA JSC, work colleagues Abraham Trujillo and Edgardo Flores for their support in completing this project.

Abstract

There are a variety of fuels that are utilized for space applications and in recent years, environmentally friendly fuels have been of interest. In the case of bipropellant rocket systems, hydrocarbon fuels have come to the attention of scientists and engineers. In particular, liquid methane was of interest in this study because of its physical and chemical advantages over other fuels, such as liquid hydrogen. Rocket engines rise to very high temperatures and to avoid catastrophic mechanical failure, a cooling system must be implemented within the engine to cool the walls. To get a better understanding of the fluid flow characteristics of liquid methane, the Center for Space Exploration Technology and Research (cSETR) at University of Texas at El Paso (UTEP) has designed and built a high heat flux test facility (HHFTF) to investigate its heat transfer characteristics. The HHFTF was developed in conjunction with Johnson Space Center (JSC) at NASA; its purpose is to simulate a cryogenic fuel going through a single channel that is exposed to high heat levels on one side. The system simulates the 1-dimensional, asymmetric heat flow experienced by the hot wall of a cooling channel in a regenerative rocket engine. A heated copper block delivers heat to small, rectangular, single channel test articles. To understand the capabilities HHFTF, a calibration method must be thoroughly defined. The goal of this study is to develop an accurate measurement of the heat being transferred to the test article within the system. By exploring a variety of different temperature measurements, and a new methodology for calculating heat flow rate, the analysis is conclusive in defining the overall heat transfer model for the system.

Table of Contents

Acknowledgements	v
Abstract	vi
Table of Contents	vii
List of Figures	ix
Chapter 1: Introduction	1
1.1 Project Overview	1
1.2 Project Objectives	2
1.3 Experimental approach.....	3
1.4 Relevance	4
Chapter 2: Literature review	5
2.1 Hydrocarbon Fuels	5
2.2 Regenerative Cooling (overview)	6
2.3 High Heat Test Facilities.....	7
Chapter 3: High Heat Flux Test Facility (HHFTF)	18
3.1 HHFTF Design Approach	18
3.2 Heating Block Modifications	25
Chapter 4: System Integration and Components	34
4.1 System measurements	35
4.2 Valves.....	40
4.3 Vacuum pumps.....	43
4.4 Electrical Components	45
Chapter 5: Methodology	49
5.1 Water Calorimetry.....	49
5.2 HHFTF Heat Transfer Model.....	50
5.3 Experimental Procedure	54
Chapter 6: Results and Analysis	58
6.1 Test Matrix Development.....	58
6.2 Heat Transfer Rate Calculations	58
6.3 Data Analysis	60

6.4	Data comparisons	65
6.5	Measurement Uncertainty	70
Chapter 7: Conclusion.....		74
7.1	Conclusion.....	74
7.2	Future Work	74
References		75
Appendix.....		76
Vita.....		89

List of Figures

Chapter 1.

Figure 1. 1: Heating Block and Test Article Assembly	3
--	---

Chapter 2.

Figure 2. 1: Example of a regenerative rocket engine	6
Figure 2. 2: Types of cooling channel geometries; milled (left), and brazed (right).	7
Figure 2. 3: A simplified schematic of the Heated Tube Facility at Glenn Research Center [5]. ..	9
Figure 2. 4: Spacing locations of the thermocouples that were placed on the HTF's test article [5].....	10
Figure 2. 5: Image of the test article geometry that was used in the NAAO [6].	12
Figure 2. 6: Overall Assembly of the high heat flux facility at Marshall Space Center [6].	12
Figure 2. 7: Assembly of the Aerojet Carbothermal Test Facility.....	14
Figure 2. 8: The three different geometries that were investigated for the HHFF [8].	15
Figure 2. 9: Temperature profile distribution for each geometry: Solid 1 (a), Solid 2 (b), and Solid 3 (c).	16
Figure 2. 10: Final design used for the HHFF; heating block (a) and the overall assembly (b) [8].	17

Chapter 3.

Figure 3. 1: Overall High Heat Flux Test Facility Assembly.	18
Figure 3. 2: An image of the main components of the heating components, including the copper heating block, test section, and aluminum cradle.	19
Figure 3. 3: Heating Block Specifications.	20
Figure 3. 4: Visual representation of heater holes in the heating block.....	20
Figure 3. 5: 0.161" x 0.0708" (.18 cm x .41 cm) channel test article.	21
Figure 3. 6: Cross-sectional view of a test article.	22
Figure 3. 7: Stainless steel stand for the HHFTF assembly.....	23
Figure 3. 8: Aluminum cradle.....	23
Figure 3. 9: CAD model of the entire HHFTF assembly.....	24
Figure 3. 10: Paper insulation between metal components.....	25
Figure 3. 11: Illustration of the heat flow in the heating block.....	26
Figure 3. 12: Location of thermocouple additions.....	27
Figure 3. 13: Temperature profile for a simulation with a constant temperature boundary.	28
Figure 3. 14: Temperature profile for a simulation with a constant heat flux boundary.	29
Figure 3. 15: Heating block with thermocouple penetration holes.	30
Figure 3. 16: Heating block with penetration hole depths.	31
Figure 3. 17: Diagram showing the thermocouple locations that were used in the HHFTF.	32
Figure 3. 18: Final heating block assembly with added thermocouples.	33

Chapter 4.

Figure 4. 1: Fully assembled HHFTF.	34
Figure 4. 2: Fluid schematic of the integrated system, including the HHFTF.....	35
Figure 4. 3: MQSS Series Omega probe thermocouples used in the HHFTF.	36
Figure 4. 4: The pressure transducer and process meter from OMEGA, used for system pressure readings.....	37
Figure 4. 5: Lesker Pirani Gauge for vacuum chamber pressure readings.	37
Figure 4. 6: Hoffer flowmeter and transmitter to get the flow rates of the fluid.	38
Figure 4. 7: Left to Right, a NI PCI-6533, a NI SCC-68, and a NI 9213 model.	39
Figure 4. 8: Image of the GUI used for the HHFTF.	40
Figure 4. 9: Quarter-turn valves used from Swagelok.....	41
Figure 4. 10: Needle valve from Dragon Valves Inc.	41
Figure 4. 11: Swagelok check valve.	42
Figure 4. 12: Photo of the fluid piping system.....	42
Figure 4. 13: EcoPure in-line Refrigeration Filter.	43
Figure 4. 14: Rocker 300 Vacuum Pump.....	44
Figure 4. 15: BOC Edwards XDS5 Scroll Vacuum Pump.	44
Figure 4. 16: Placement of Scroll vacuum pump in the HHFTF.	45
Figure 4. 17: Resistive cartridge heaters from Gordo Sales Inc.	46
Figure 4. 18: Arrangement of cartridge heaters inside the copper block.	46
Figure 4. 19: Cartridge heaters secured with Resbond.	47
Figure 4. 20: Solid state relay used (left) and the switch used to control the power (right).	48
Figure 4. 21: Extech Quad output DC power supply.....	48

Chapter 5.

Figure 5. 1: Summary of Heat Transfer Analyses completed.....	50
Figure 5. 2: Illustration of the linear model used for variable area.....	52
Figure 5. 3: Boundaries for 1-D conduction dependent on geometry [10].....	53
Figure 5. 4: Illustration of the boundaries in the model.....	53
Figure 5. 5: Simplified Fluid Schematic of the HHFTF.	56

Chapter 6.

Figure 6. 1: Block with labeled axes used in conduction analysis.....	59
Figure 6. 2: Example of Overall Temperature Results with increasing Block Temperature.....	61
Figure 6. 3: Actual Block Temperature readings, as Temperature increases.	62
Figure 6. 4: Temperature results of Test 3 at 150°C.....	63
Figure 6. 5: Analysis approach for Test 3.....	64
Figure 6. 6: Convective Heat Transfer Results.	66
Figure 6. 7: Conductive Heat Transfer Results.....	67

Figure 6. 8: Conduction and Convection Heat Transfer comparison.	68
Figure 6. 9: Trendline of all Q_Ratio values found.	69
Figure 6. 10: Q_convection vs. dT of Block.....	70
Figure 6. 11: Test Section and Cradle Assembly with paper insulation.	71
Figure 6. 12: Resistance Network used for analysis.	72
Figure 6. 13: Q_loss due to radiation as Block Temperature increases.....	73

Chapter 1: Introduction

1.1 Project Overview

In recent space systems, scientists are looking towards different options for propellants that will be able present endurance in longer flight durations and more reliability than current systems. In the case of large space launchers, liquid bipropellant systems have been widely used for rocket engines. There has been interest in environmentally friendly propellants for use in space applications and hydrocarbon fuels have been recognized as a good candidate due to their definitive physical and chemical advantages over other fuels. Methane (CH_4), in particular, is being investigated as the propellant for liquid methane-liquid oxygen ($\text{CH}_4\text{-O}_2$) bipropellant rocket systems. Its advantages include high density, desirable storage properties, low toxicity, and thrust efficiency [1]. There is a fair amount of data readily available for heat transfer characteristics of gas methane but there is not a lot of empirical data offered for liquid methane.

In rocket engine design, temperature variation between the combustion chamber and the exit nozzle is significant and for this reason, a cooling system for these engines must be properly designed. Regenerative (regen) cooling is a cooling method of much interest because of its advantages over other methods primarily by utilizing the available fuel for both cooling and combustion within the system.

Over the past few years, the Johnson Space Center (JSC) of the National Aeronautics and Space Administration (NASA) has been developing the design of an autonomous, planetary lander called Project Morpheus which will use a $\text{LCH}_4\text{-LOX}$ propellant system for its main and navigation thrusters [2]. The Center for Space Exploration Technology and Research (cSETR) at the University of Texas at El Paso (UTEP) has built a High Heat Flux Test Facility (HHFTF) inspired by this project to investigate the heat transfer characteristics of liquid methane.

The HHFTF was built to simulate the high temperature environment that cooling channels are exposed to in regenerative (regen) cooling rocket engines. Cryogenic fuel going through a regen engine's cooling channel is simulated in the HHFTF, by flowing liquid methane through a single channel that is exposed to high heat levels on one side. This simulates the single-sided, asymmetric heat flow experienced by the hot wall of a cooling and allows the fluid properties of liquid methane to be characterized and documented for future reference. The facility was designed and developed between 2009- 2011 and has been functioning over past few years for experimental use.

To ensure that the HHFTF is operating under repeatable and sustainable conditions, a calibration method must be clearly defined. Only when there is a clear understanding of the HHFTF's capabilities, can the system's assertions be verified. The goal of this study is to develop an accurate measurement of the heat being transferred to a single channel test article placed in the system. By placing supplementary sensors and implementing a unique approach to calculate heat transfer, the results will be used to analyze the system's heat transfer model.

1.2 Project Objectives

In the design of any experimental setup, it is fundamental to understand the system's capabilities and whether the experiments that are performed have credibility and repeatability. Calibration methods are essential to ensure accurate measurements. A specific water calorimeter procedure and analysis was developed, specifically for the HHFTF, to investigate the heat transferred in the system.

The HHFTF contains a solid copper block that is heated with cylindrical resistive heaters. The heat from the copper block is directed heat to small rectangular test articles that are placed on top of the block, directly in the line of travelling heat. The heating conditions are similar to

those are experienced by the cooling channels of a rocket engine, as specified in section 1.2, and define these constraints define the boundaries of the system. This heating assembly can be seen below, in Figure 1.1.

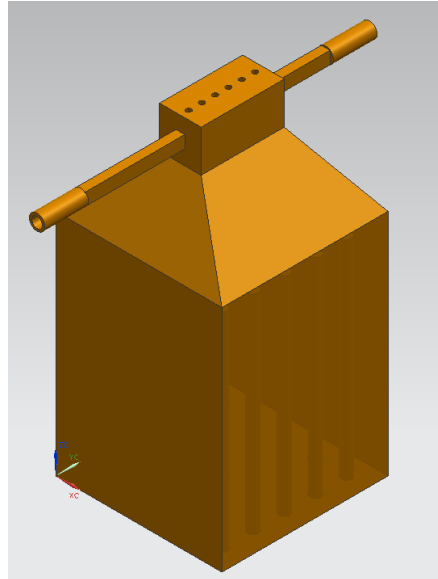


Figure 1. 1: Heating Block and Test Article Assembly.

The test articles contain a single channel geometry based on cooling channel designs that are truly used in regen engines. The design of the HHFTF allows the assumption that flow is 1-dimensional to be used. The measurement of the 1-dimensional heat flux going into the test article is essential for precision in data analysis. By using various heat transfer calculations, a calibration curve can specify these properties for future reference.

1.3 Experimental approach

Two approaches of heat transfer analysis were used, including a convection-based analysis, and a conduction-based analysis. One uses the channel fluid flow characteristics and the other, defines the heating characteristics based on the geometric constraints, respectively.

Ultimately, the basis of the project compares and evaluates the results between the two different heat transfer analysis methods.

Since its design and development, modifications have been made to the HHFTF setup to more accurately reflect the properties of the heating system under testing conditions. Mainly, temperature sensors were added at various locations within the HHFTF; the different constraints of the experimental setup are considered to measure and analyze the heat being transferred between the different components. The sensors in the HHFTF tests, including temperature, flow rate, and pressure readings. By monitoring the activity of the HHFTF as a test progresses, the heating capabilities of the system were recorded for analysis.

The HHFTF was designed with English units in mind, however, the units used to measure heat and energy uses metric. Therefore, unit conversions had to be implemented to display the correct values for calculations. The remainder of the report will refer to both types by relevance and importance to the topic being discussed.

1.4 Relevance

The HHFTF was continuously used to investigate liquid methane and the conclusions from this new approach can verify the validity of the analysis in previous studies. There are many research facilities that use high heat levels to simulate various conditions. By defining a specified model for calibration, the methodology developed in this project can be applied to other geometries and specifications for future design; this includes other high heat flux systems that are similar in design and approach.

Chapter 2: Literature review

2.1 Hydrocarbon Fuels

Scientists have been looking for different propellants that can be used for space applications that are less costly in handling and safety than current systems; there has particularly been an interest in hydrocarbon fuels. A familiar bipropellant system for rocket engines is liquid oxygen-liquid hydrogen (LOX/LH₂) engines, which have worked successfully for recent systems. A disadvantage, however, is that these systems are difficult to maintain because of the handling requirements of hydrogen. Hydrogen has a low density (0.0899 kg/m³) requires large storage tanks. It also has a cryogenic storage temperature (-253 °C) that is much lower than the systems' oxidizer, LOX (at -183 °C) [1]. An alternative to the LOX/LH₂ bipropellant system is replacing hydrogen, with a hydrocarbon fuel. In particular, liquid methane was the fuel of interest when designing the HHFTF because of several its definitive physical and chemical advantages over other fuels.

Methane has a high density that allows more fuel to be stored in a smaller volume. The storage properties of liquid methane (-161 °C) are quite similar to that of LOX (-183 °C) which is the oxidizer used in CH₄-O₂ bipropellant systems [1]. The combustion gases that are created by the reaction (CO₂ and H₂O) are less toxic than other mixtures (H₂-O₂ system). In-situ mining is another advantage of methane; this is a chemical that is bountiful in the universe and it is known that lunar and other space rocks, such as meteors have it present on their structure [1]. This also allows for methane to be mined from space without requiring extra storage on a vehicle and lightweight vehicles are more efficient for space applications.

2.2 Regenerative Cooling (overview)

The rocket sizes that are of interest in this study are rather large, and understandably work at very high temperatures. Fuel, in large rocket engines, is held as a low-temperature cryogenic liquid to maximize available storage space, and therefore can be used as a coolant for the engine. Regenerative cooling has become a desirable option rather than other cooling methods such as dump or film cooling. These other cooling methods use part of the stored fuel as a coolant for the system but is expelled as waste after use. Regenerative cooling, conversely, uses a system where the propellant serves a dual purpose. In regenerative cooling, the cryogen is sent along multiple cooling channels that are designed along the surface of the engine to cool the walls; it is then sent into the combustion chamber to combust and produce thrust [3]. An image of a regenerative rocket engine can be seen in Figure 2.1.

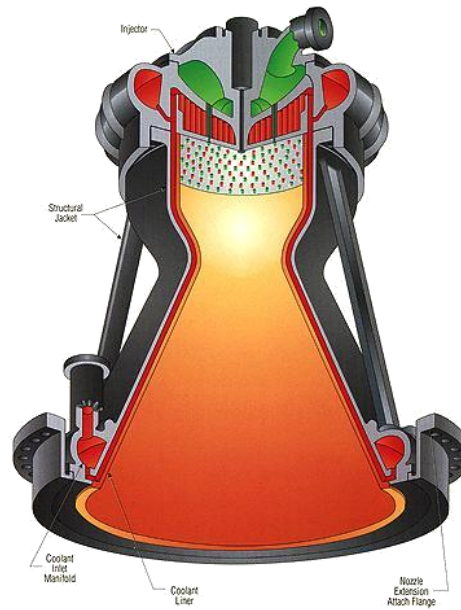


Figure 2. 1: Example of a regenerative rocket engine.

There are different types of cooling channels that have been investigated to optimize cooling capabilities including brazed channels, which have a circular cross-sectional geometry,

and milled channels, which have a rectangular geometry. Figure 2.2 shows an example of the types of cooling channel geometries used in rockets.

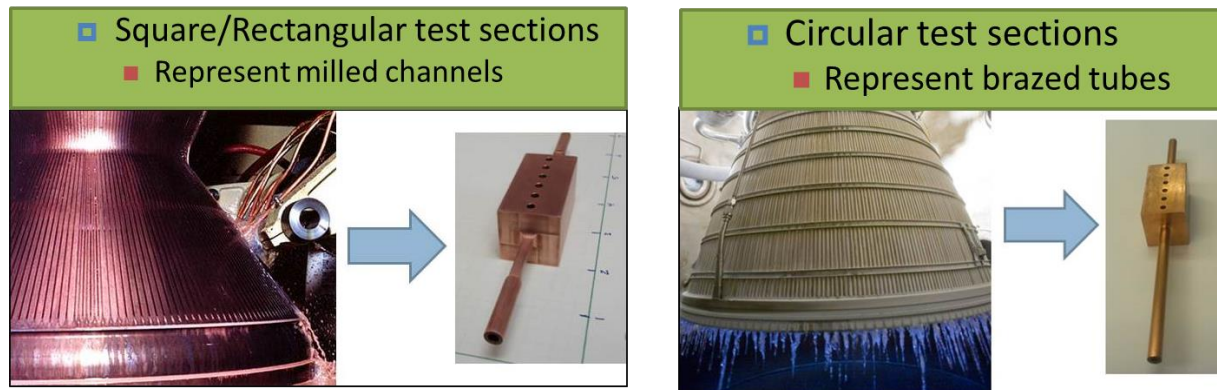


Figure 2. 2: Types of cooling channel geometries; milled (left), and brazed (right).

When combustion occurs, maximum efficiency is reached when the fuel is fully gaseous and this is another advantage of regenerative engines. The process of cooling the engine wall heats the fuel so it is gaseous when it is injected for combustion [3].

2.3 High Heat Test Facilities

High Heat flux facilities were developed by several different laboratory facilities to study heat transfer characteristics of various liquid propellants. Several facilities are specifically designed to simulate the cooling channels of regenerative rocket engines; these systems were of interest because of the nature of the project. These designs found fluid heat transfer properties by directing it through a heated channel via internal forced convection. The design for these systems accurately simulated the extreme environments experienced by the cooling channels in pressure, temperature, and heat flux. The heating method used for these high heat flux facilities can be divided into two types: resistive and conductive heating methods. The heat flow in resistive heating is described as circumferential, while flow of heat in conductive heat transfer involves one-sided, asymmetric flow.

2.3.1 Resistively heated tube facilities

Resistive heating is also known as ohmic or joule heating; it is a heating process that is based on applying a current to a conductive metal. Using the basic idea of Joule's First Law, $Q \propto I^2 * R * t$, the amount of energy released as heat, is proportional to the current squared [4]. The resistance of the conductor determines how much heat flux is applied to the. Essentially, when a current is applied to the conductive material, energy is released as heat and becomes an exothermic system. Although the current applied allows the heat flux of the system to be accurately defined, high heat fluxes require extremely high power levels. This presents a safety danger and raising temperature using a high current may also lead to uncertainty due to electrical effects on data records [2]. In the case of simulating cooling channels, the current is applied directly to the channel and circumferentially heats it throughout the geometry. Therefore, heat is evenly distributed along the surface of the channel. There are several high heat flux facilities that use this method including research that was performed at NASA Glenn Research Center's Heated Tube Facility, and a study performed by NASA Marshall Space Flight Center and Rocketdyne.

Glenn Research Center Heated Tube Facility

In 2010, a study was performed at NASA Glenn Research Center (GRC) to investigate the heat characteristics of liquid and two-phase methane. The overall goal was to understand how this fuel would respond under extreme conditions that it would experience in the cooling channels of a rocket engine [5]. GRC had performed previous studies of fuels going through resistively heated tubes in the 1960s, and again 1991, using a facility known as the Heated Tube Facility (HTF). A simplified schematic of the facility can be seen in Figure 2.3. The investigation in 2010 used the same heated tube facility to analyze cryogenic methane.

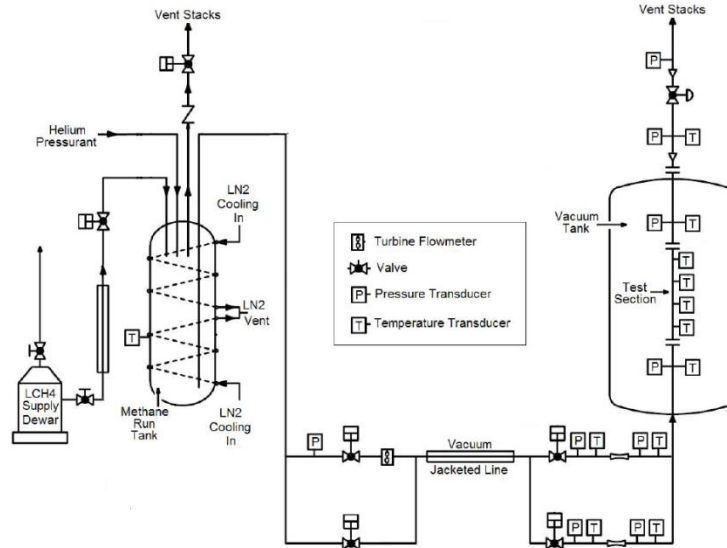


Figure 2. 3: A simplified schematic of the Heated Tube Facility at Glenn Research Center [5].

The HTF simulates the conditions in pressure, temperature, and heat flux of a cooling channel. It consists of a test article that contains a single cooling channel tubes, made of Inconel 600. There were three separate test articles, each with a specified cross-sectional geometry. The test article is placed inside a vacuum chamber to avoid heat losses due to convection and provide a safe environment for the people performing tests in case of fuel leaks or other hazards. Copper bus bars were attached to the tubes to provide the resistive power to the test article. A high current, up to 1500 amps (at 100 volts), went through the channel to heat it up to the desired temperature and heat flux. The heat flux in the system reached up to 10.1 MW/m^2 and the channel temperature went up as high as 726°C [5]. The pressure of the fuel applied to the system was controlled with two cavitating venturis, and flow rate was measured with a flowmeter rated for methane.

The temperature along the cooling channel, as the fuel went through it, was monitored with a series of 15 thermocouples that were spot-welded to the side of the channel, each placed at

an incremental spacing $\sim 0.5''$ (1.27 cm) along the channel. The position of these thermocouples and an overall image of the test assembly can be seen in Figure 2.4.

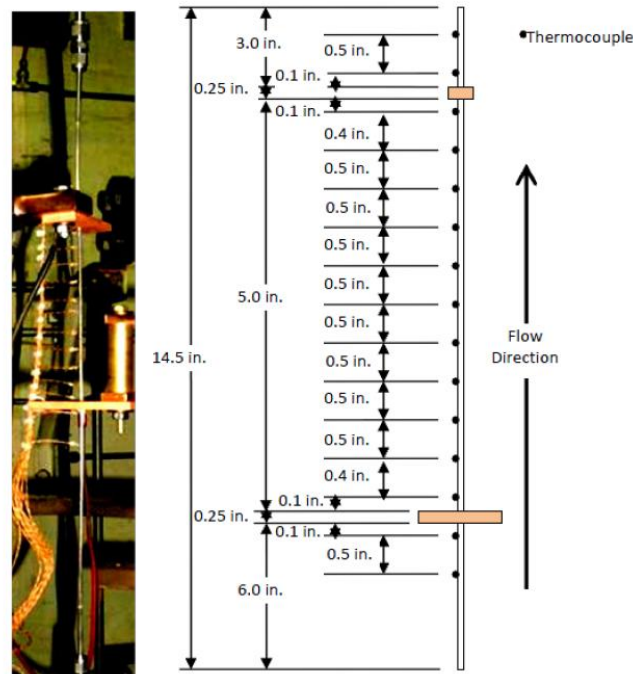


Figure 2. 4: Spacing locations of the thermocouples that were placed on the HTF's test article [5].

There were a variety of tests that were performed, including a test that incrementally increased the heat flux into the channel. This test allowed the study to find and analyze the critical heat flux of methane, which is defined as the onset of film boiling.

Marshall Space Flight Center and Rocketdyne Electrically-Heated Tubular Test

The interest in more environmentally friendly fuels has led to many studies regarding hydrocarbon fuels. In the mid-1980s, Rocketdyne, in conjunction with NASA Marshall Space Flight Center, performed a 12 month investigation of the heat transfer characteristics of liquid methane (LCH₄) and liquid natural gas (LNG), which is 94% methane [6]. The goal of the project was to understand the coking thresholds, heat transfer properties and cooling capability

(convective correlations) of these fuels. A previous study performed by Rocketdyne, used stainless steel channels that were resistively heated to simulate the flow and find heat characteristics. However, due to the channel's material properties, there were limited heat fluxes that could be applied to the system and coking behavior was not noticeably observed. For this reason, the present study selected pure copper, which is known to have a high thermal conductivity. Copper allowed the test channel to be exposed to very high heat fluxes, which is very likely for future high pressure chambers in rockets.

A high heat facility using single channel copper-base test articles was developed at the Rockwell North American Aviation Operations (NAAO) Aerothermal Laboratory. This system was modeled to aid in research for reusable and high performance rocket booster engines by using copper based alloys for the test articles, similar to those present in the chamber of the Space Shuttle Main Engine (SSME) [6]. The surrounding environment of the facility also simulated those present in the SSME. This facility consisted of a heated channel that measured temperature and pressure readings as a fuel flowed through it. The tests included of a variety of flow rates, pressures, and heat fluxes to accurately characterize the flow. The channel in the test article was a bimetallic tube made of OHFC copper with a surrounding Inconel K-500 reinforcement. It consisted of a row of thermocouples that measured and recorded the temperature of the flow at a specified distance increment, as seen in Figure 2.5.

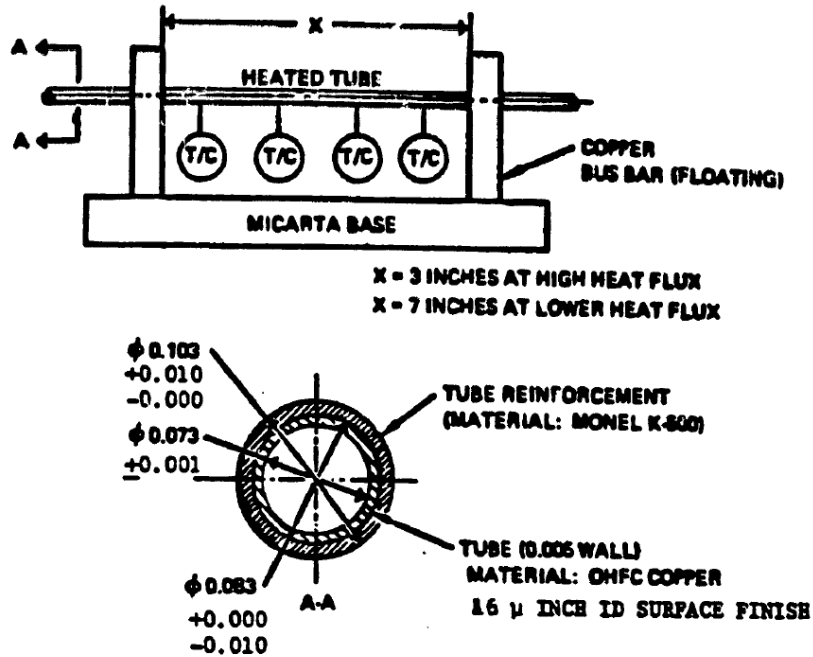


Figure 2. 5: Image of the test article geometry that was used in the NAAO [6].

Wall temperatures inside the channel ranged from 316 to 482 °C, while working fluid pressures went up as far as 31 MPa. Fluid velocities ranged from 55.2 to 238.0 m/s. Three arc reactors, each rated at 2000 amps, were used to resistively heat the bimetallic tubes up to a maximum constant heat flux of 139 MW/m². The overall assembly of the setup can be seen in Figure 2.6.

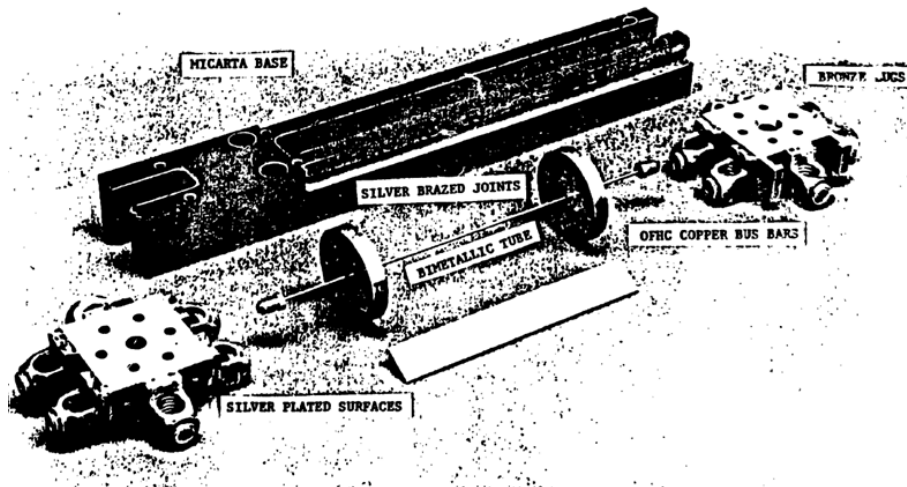


Figure 2. 6: Overall Assembly of the high heat flux facility at Marshall Space Center [6].

2.3.2 Conductively heated tube facilities

Heat flux facilities that use conductive heating operate with a system where the pre-heated component is made in contact a test article to ensure a constant contact area and constant heat flux delivery. This method, unlike resistive heating, heats the channel asymmetrically from one side and can be better compared to the hot and cold walls that a cooling channel would be exposed to in a regenerative engine [7]. Because there is no electrical current directly affecting the test article, there is no risk of having electrically driven chemical phenomena, which is possible with the high currents used in resistive heating. Resistive heating may lead to material degradation because of high electrical currents which is not an issue in conductive heating [4].

Studies have been made to design an effective conductive heating facility that will efficiently heat a specified test article including a Carbothermal Rig used at Aerojet TechSystems and research performed by the Air Force Research Laboratory (AFRL). The HHFTF used at cSETR was designed with much influence from the conductive heating facilities described below.

Aerojet Study

In the late 1980s, a study was performed at Aerojet Technical Systems Co. regarding the material compatibility of various hydrocarbon fuels with potential metal liners for combustion chambers. The aim of this study was to define and evaluate the interaction between these materials, and develop a solution to avoid extreme corrosive damage in combustion chambers [7]. The incentive for this project came from a previous study performed by the United Technologies Research Center and the Rockwell International Rocketdyne Division. When resistive heating was used in these studies, severe copper corrosion and carbon disposition was found and led to examine these characteristics [7]. The metals of interest in the Aerojet study

were copper-based and included OFHC, NASA-Z, and ZrCu coppers; the hydrocarbon fuels that were tested included Mil-Spec RP-1, n-dodecane, propane, and methane.

To investigate these reactions, the Aerojet Carbothermal Test Facility (ACTF) was developed; this high heat flux facility was based on conductive heating. As seen in Figure 2.7 below, the facility consists of a large, solid copper block that was heated using imbedded cartridge heaters. The heat is directed to a small test article that consists of a milled square channel that the fuel flows through. Both static and dynamic tests were performed with the ACTF. Static tests consisted of running the fuel through the block at a constant pressure and temperature for long durations; dynamic tests simulated the pressures, temperatures and heat fluxes the combustion chamber a regen engine would experience. Pressures of up to 24.1 MPa, temperatures up to 499°C, and heat fluxes as high as 86.7 MW/m² were studied [7].

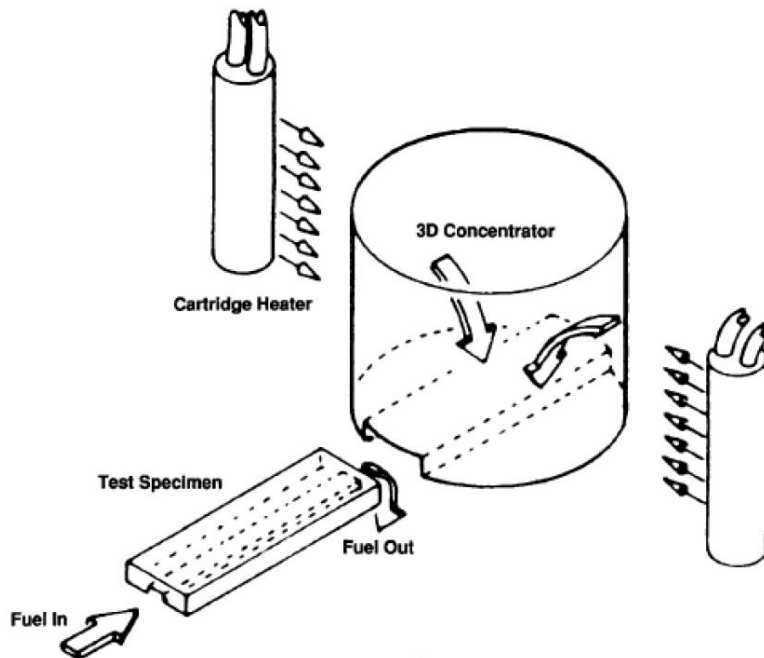


Figure 2. 7: Assembly of the Aerojet Carbothermal Test Facility.

Air Force Research Laboratory

The Air Force Research Laboratory (AFRL) built a High Heat Flux Facility (HHFF) from 2004 to 2007 to study the heat transfer characteristics of hydrocarbon fuels. This project can be seen as an extension of the Aerojet study described above; the facility's design was highly influenced by the Aerojet study, which also uses conductively transferred heat from a copper solid to a small test article. The fuel of interest in this study was RP-2. The AFRL's main goal was to design and develop a heating rig that would deliver heat to a test article effectively. Their approach was to design and build various heat source geometries and determine which option would best deliver heat to the test article [8].

There were three separate solid metal geometries that were observed in the experiment.

The geometries were designed and analyzed by using CFD++ to find how heat conduction travelled through the solid. The convective heat transfer rate was set as a boundary condition for the simulations. The three different geometries can be seen in Figure 2.8.

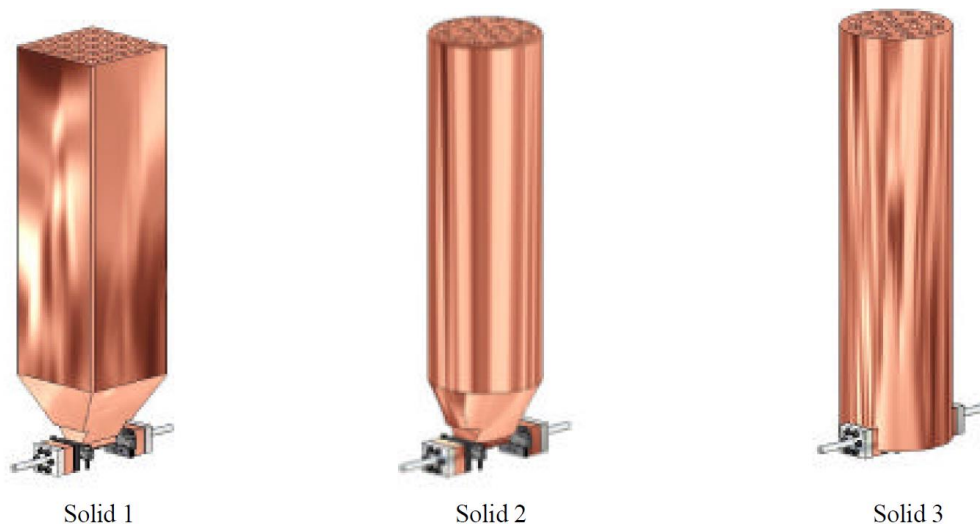


Figure 2. 8: The three different geometries that were investigated for the HHFF [8].

Solid 1 was a solid rectangular block that directed heat to a trapezoidal pyramid with a taper that specifically matched the dimensions of the test article. Solid 2 was a cylinder that has a conical shape to direct heat to the test article. Solid 3 was a cylinder that encompasses the test article and directs heat by surrounding the top and sides. Solids 1 and 2 are geometrically focused to deliver heat to the test section, while Solid 3 is the only design that has an embedded test section; this design is similar to Aerojet's Carbothermal Test Facility. A large portion of each solid was designed to hold resistive heating cartridges that would heat the test section; it was ensured that each solid had sufficient space between the heaters and the test article to allow for even thermal diffusion into the test article [8].

A Steady state finite element simulation was performed for each design; the temperature profile for each Solid is shown in Figure 2.9. The overall goal of this simulation was to see which geometry would evenly distribute heat to the test section with a higher heat flux. Based on these results, it was decided that the final heating block would be a hybrid model that incorporates both Solid 1 and Solid 3. The figure shows a cross sectional view of the temperature profile of each block, cut at the XZ plane.

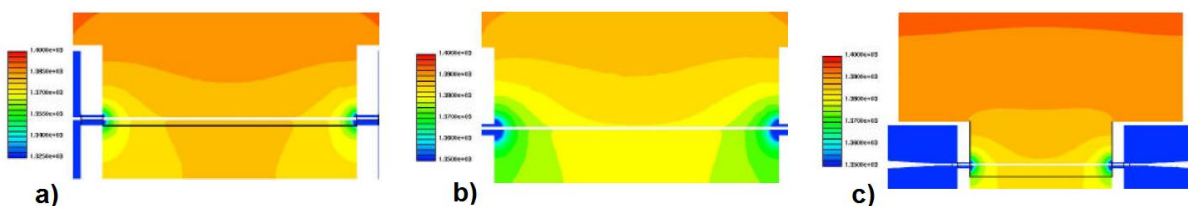


Figure 2. 9: Temperature profile distribution for each geometry: Solid 1 (a), Solid 2 (b), and Solid 3 (c).

Based on the results from these simulations, a design that incorporated Solid 1 (trapezoidal prism) and Solid 3 (embedded test section) was selected. The final block design, as well as the full assembly of the HHFF developed at AFRL, can be seen in Figure 2.10. A major advantage

of this design was that the test articles were made to be exchangeable which allows for various channel geometries to be applied to the heating block

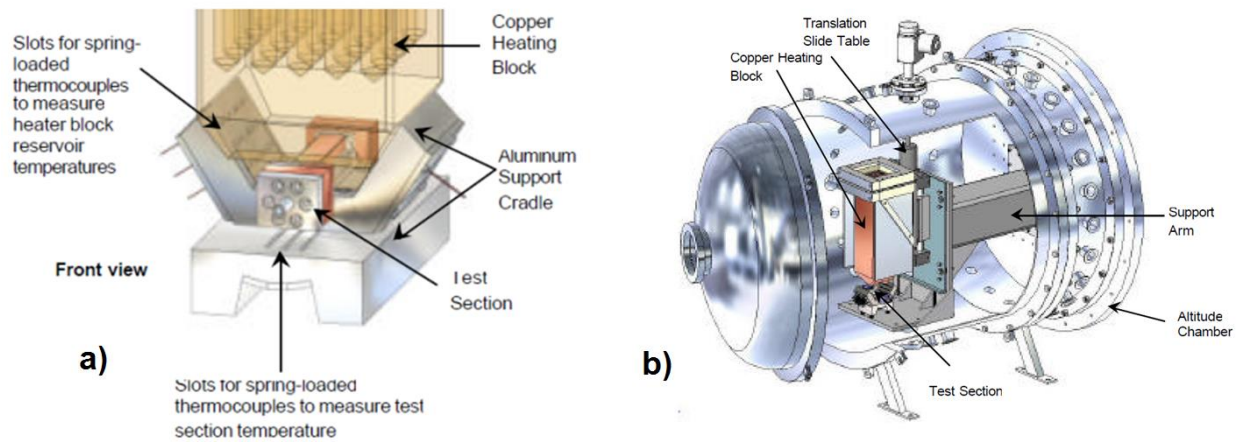


Figure 2. 10: Final design used for the HHFF; heating block (a) and the overall assembly (b) [8].

Chapter 3: High Heat Flux Test Facility (HHFTF)

3.1 HHFTF Design Approach

The high heat flux test facility (HHFTF) was designed and developed at cSETR between 2009 and 2011 and is a system that studies heating characteristics of fluids by supplying a constant heat flux to a test article through steady heat conduction. The facility consists of a solid copper block, with a tapered trapezoidal portion. It is heated using cylindrical resistive heaters that are placed inside holes at the bottom in the block. The design for this geometry was highly influenced by the High Heat Flux Facility that was made by the Air Force Research Laboratory [8]. Heat from the block is directed heat to small rectangular test articles that are placed on top of it. The contact interface between the block and test article is a flat plane to encourage even heat distribution. The entire setup is placed inside a vacuum chamber to resist undesirable heat transfer effects such as convection. The assembly of the HHFTF can be seen in Figure 3.1.

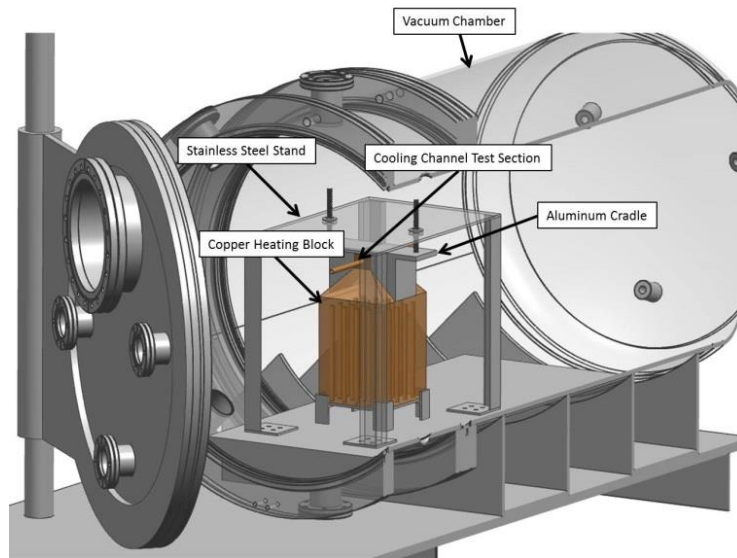


Figure 3. 1: Overall High Heat Flux Test Facility Assembly.

A more detailed view of the heating block and test article can be seen in Figure 3.2. The test articles consist of a single cooling channel and were designed to be exchangeable so various

channel geometries could be used without replacing the heating block. The cradle is placed on top of the test article to secure contact between the surfaces.

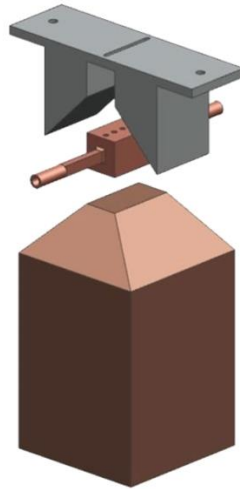


Figure 3. 2: An image of the main components of the heating components, including the copper heating block, test section, and aluminum cradle.

The facility utilizes influence from both conductive and resistive heating methods. While resistive cartridge heaters are used to heat the copper block, the test article is heated with the conductive heat transferred at the block-test article contact interface, to evenly distribute a heat flux into the channel.

3.1.1 Components

Copper Heating Block

The heating block is a solid metal block made of C12200 copper and is used as the thermal concentrator of the setup. The overall dimensions of the block are 4" x 4" x 7" (10.16 x 10.16 x 17.78 cm³). It has a 4" (10.16 cm) square cross-section with a tapered trapezoidal pyramid at the top that is 1.5" (3.81 cm) high. The taper is sized to fit the rectangular test article on top of the block with an area of 2" x 1" (5.08 x 2.54 cm²). Copper was selected as the

block material because of its high thermal conductivity rating, at 231 Btu/(hr*ft*F) or 401 W/(m*K). An image of the block and specified dimensions can be seen in Figure 3.3.

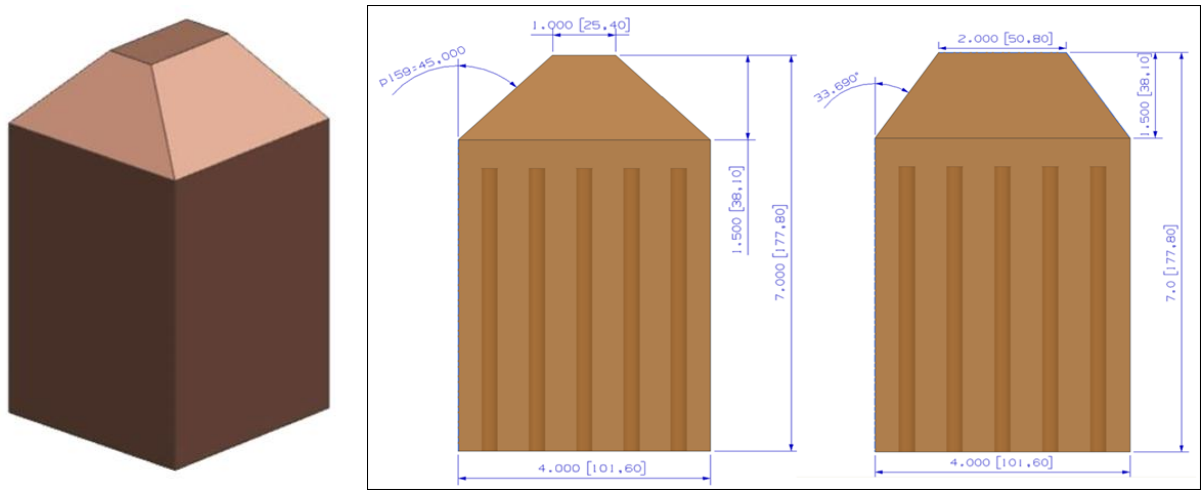


Figure 3. 3: Heating Block Specifications.

There are 25 holes inside the square copper block on the bottom face that allow cylindrical cartridge heaters to be placed inside to heat the block; Figure 3.4 shows a representation of these holes. For the sake of available power and current in the cSETR laboratory, the HHFTF uses a total of 18 heaters.

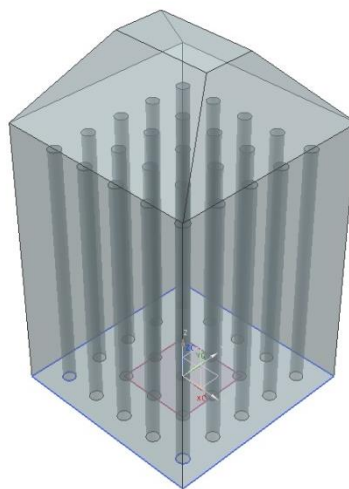


Figure 3. 4: Visual representation of heater holes in the heating block.

Test Article Design

The purpose of the test articles is to simulate a portion of a cooling channel and consist of a single channel geometry that is a sub scale model to cooling channels that are used in regenerative rocket engines. A test article can be seen in Figure 3.5. The heated portion of the test article is a rectangular prism with a 2" x 1" x 1" (5.08 x 2.54 x 2.54 cm³) geometry that fits onto the top of the block seamlessly.



Figure 3. 5: 0.161" x 0.0708" (.18 cm x .41 cm) channel test article.

The overall geometry was selected because it allowed different test articles to be interchangeable fairly easily. The test sections take into consideration the fluid temperature using 6 thermocouple ports that are placed very close to the fluid flow of the channel (skin temperature). These thermocouples do not have direct contact with the fluid because that could affect the flow pattern within the channel. The channels are small so the boundary layer effect needs to be considered. There are, however, thermocouples that read the inlet and the outlet test section fluid temperatures. These are directly in contact with the fluid but are far enough from the test section to not affect the flow pattern. The inlet section of the channel is designed for an entry length and ensures that the data recorded from the test article is fully developed flow using $\text{Length} = 10 \times (\text{channel hydraulic diameter})$. Figure 3.6 shows an image of where the thermocouples are located on the test section.

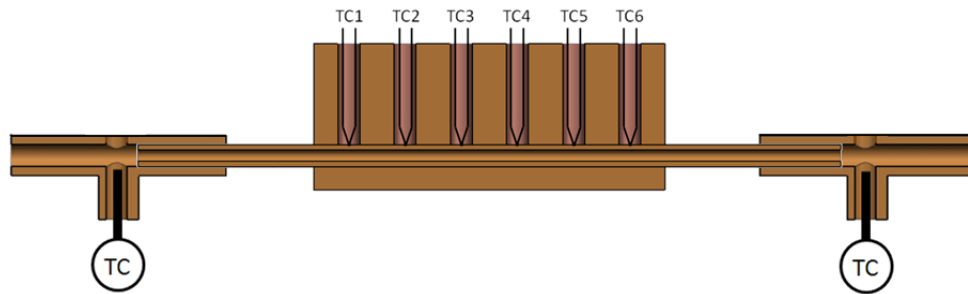


Figure 3. 6: Cross-sectional view of a test article.

For the purpose of this experiment, only one test section was used with a cross sectional geometry of 0.161" x 0.0708" (.18 mm x .41 mm), width*height. The hydraulic diameter of this channel is ~0.098", or ~2.5 mm. The channel can be seen in Figure 3.5; it was designed and developed by NASA White Sands Test Facility and represents the cross section located near the engine's combustion chamber before entering the nozzle. This rectangular geometry was selected for this study because there is a good amount of data to compare against, if needed, and it is closest to the true scale of a cooling channel for a regen engine that was being designed at JSC. The geometry has been used by NASA as a working aspect ratio for optimal cooling capabilities.

The interface between the block and the test article is a flat plane on either side to contribute to even heat flow and ease of machinability. It is checked often to make sure there is no sign of oxidation between the surfaces. In the case of oxidation, the surfaces are carefully polished with a very fine grade of sandpaper.

Additional Components

The heating block and test article are set in place with a stainless steel stand that was designed to hold all the components together. The stand can be seen in Figure 3.7; the block is placed on the hinges upright and a hole is cut in the stand so the heater wires are not strained.

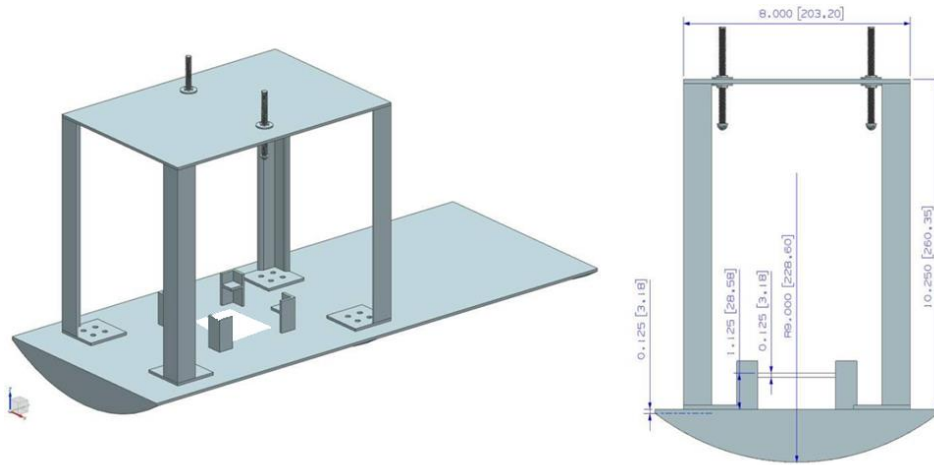


Figure 3. 7: Stainless steel stand for the HHFTF assembly.

The test article is secured with an aluminum (Al-6061) cradle, as seen in Figure 3.8, which presses the test section onto the heating block to guarantee complete flush contact between the surfaces. A penetrating thermocouple was added to the cradle to get an accurate reading of its core temperature as a test progresses.

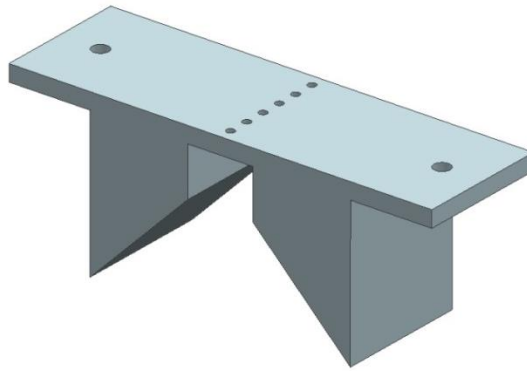


Figure 3. 8: Aluminum cradle.

The entire stand and heating assembly is placed inside a vacuum chamber. A CAD model of the complete assembly of the HHFTF inside the vacuum chamber can be seen in Figure 3.9. The tests are performed in vacuum to minimize any losses due to convection, based on

previous experiments within the HHFTF, the heat loss due to radiation were less than 2.5% of the total contribution of heat and considered negligible [9]. From this, it can be concluded that the heat transfer between the components of the HHFTF is strictly between the heating block and the test article and is through conduction.

Vacuum chamber

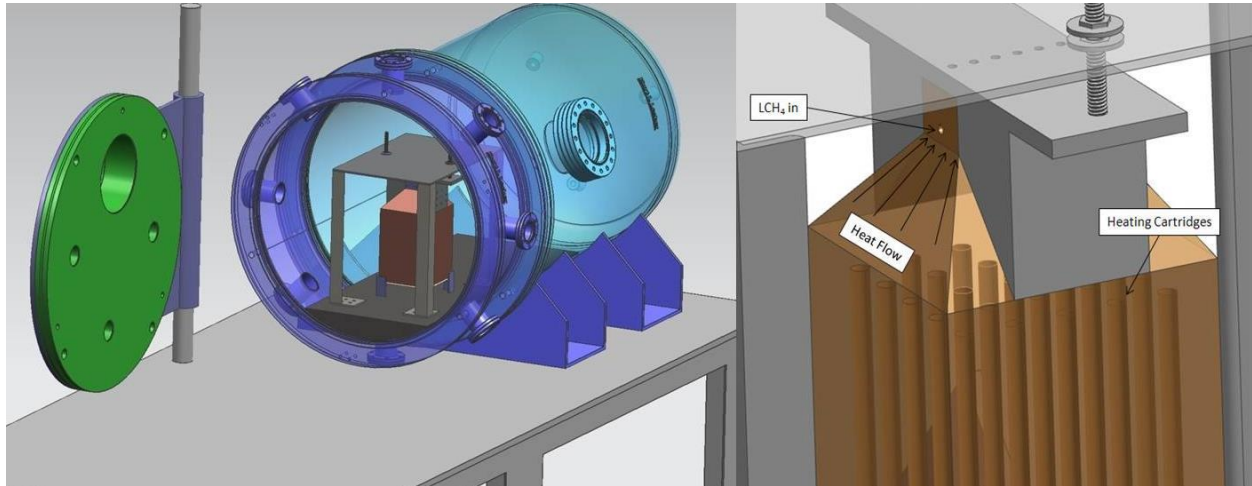


Figure 3. 9: CAD model of the entire HHFTF assembly.

Placing the system in a vacuum chamber avoided heat loss due to convection, however, there were several locations between the components where metal was in contact with metal, which caused conduction heat loss and loss of heat flux values. Notably, the heating block was in contact with the stainless steel stand and the cradle was in contact with the test section. High temperature paper insulation, Unifrax 1600 Paper, was placed between the metal- metal contact surfaces to avoid any unwanted conduction heat transfer. The insulation between the components can be seen in the photo below, in Figure 3.10.



Figure 3. 10: Paper insulation between metal components.

3.2 Heating Block Modifications

After its development in 2011, a water calorimetry procedure was developed to define the heat transferred between the heating block and the fluid inside the channel. However, this method proved to be imprecise and several important factors were not specifically defined as boundaries. To improve the method used to measure the heat in the system, temperature sensor readings were added, including thermocouples that were placed at precise locations. These sensor additions required geometric and heat transfer analysis of the geometric boundary conditions that are already present in the system; tangibly, several components required machining to accommodate the changes.

3.2.1 Design Alterations

The copper block is a square prism that has a trapezoidal pyramid that tapers to the size of the test article. Because the flow is understood to be evenly distributed in the square portion of the block geometry, a heat transfer relationship of heat flow to the test article can be found using the

trapezoidal pyramid; Figure 3.11 describes the flow of heat in the block. The trapezoidal portion can be viewed as an area-changing plane with respect to the vertical axis (x-axis).

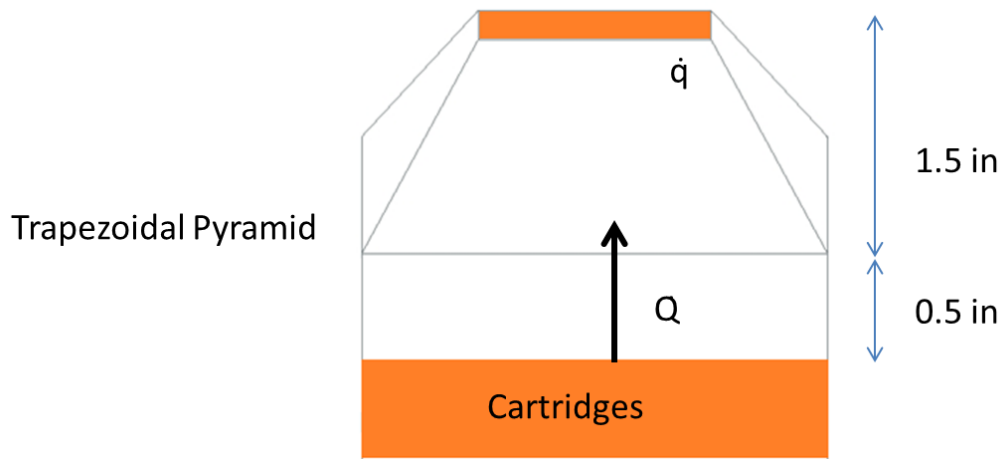


Figure 3. 11: Illustration of the heat flow in the heating block.

By specifying the temperature at two different x-locations within this portion, between the start of the trapezoidal portion and the test article interface, a 1-D heat transfer relationship will result in a heat flux measurement for the block [10]. This concept is described in more detail in section 5.2.2. Previously, the temperature of the heating block was determined by four probe thermocouples that were pressed against the surface of the block in the trapezoidal region. Unfortunately, there was a wide variation between these temperature readings and resultantly was not a good representation of the block temperature. Thermocouples that penetrate the block at different heights, as represented in Figure 3.12, will get a more accurate reading of the block's core temperature because it is directly in path of flow and was selected as the method to attach the sensors to the block.

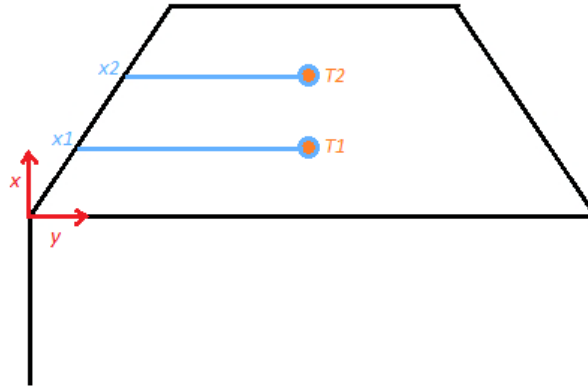


Figure 3. 12: Location of thermocouple additions.

3.2.2 Finite Element Simulations

Steady state thermal simulations were performed on the heating block and test section assembly to observe how the heat would move through the trapezoidal portion and into the test section using ANSYS Workbench 14.5. This section was of interest because the square portion has a relatively easily predicted heat flow; the square prism at the bottom of the block is exposed to the heat from the cartridge heaters which are arranged to evenly provide heat flow. The goal of the simulations that were performed was to observe the temperature distribution of the block when implementing steady state boundary condition to the block and test section geometry. By finding a temperature profile in this portion, critical x-locations for the thermocouples can be found to get a delta temperature that will allow a heat flux, $Q(x, T)$, value to be calculated for analysis.

Several steady state thermal simulations were performed using a variety of boundary conditions at the different surfaces, some of the results can be seen below. Because of the even heat flow predicted in the square portion of the block, the block was cut and given a single boundary at the bottom face going into the trapezoidal portion. Figures 3.13 and 3.14 show the

temperature profile results for a constant temperature and constant heat flux exposure at the bottom face, respectively.

A coupling temperature boundary was placed at the contact interface between the block and the test article. A low radiation rating was applied to all open surfaces, including inside the channel, this is when there is no fluid running through the channel and vacuum has been pulled inside the lines. The trapezoidal portion is known to have a height of 1.5"; using the simulations and the geometric constraints, the simulations show a temperature profile that is generally one-dimensional and flat.

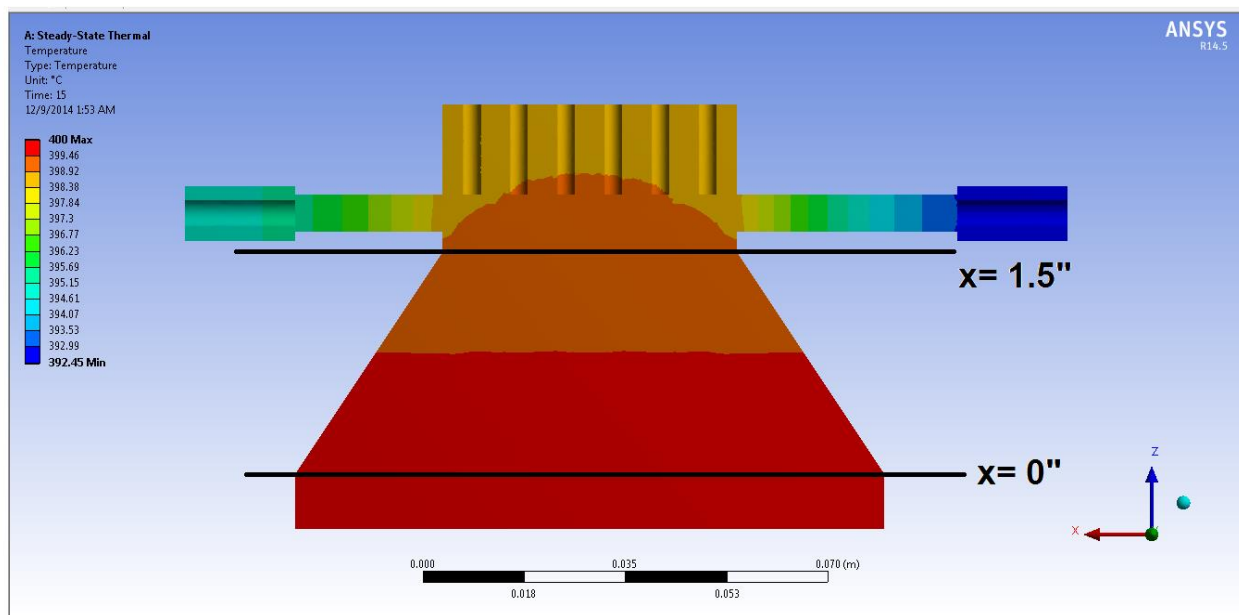


Figure 3. 13: Temperature profile for a simulation with a constant temperature boundary.

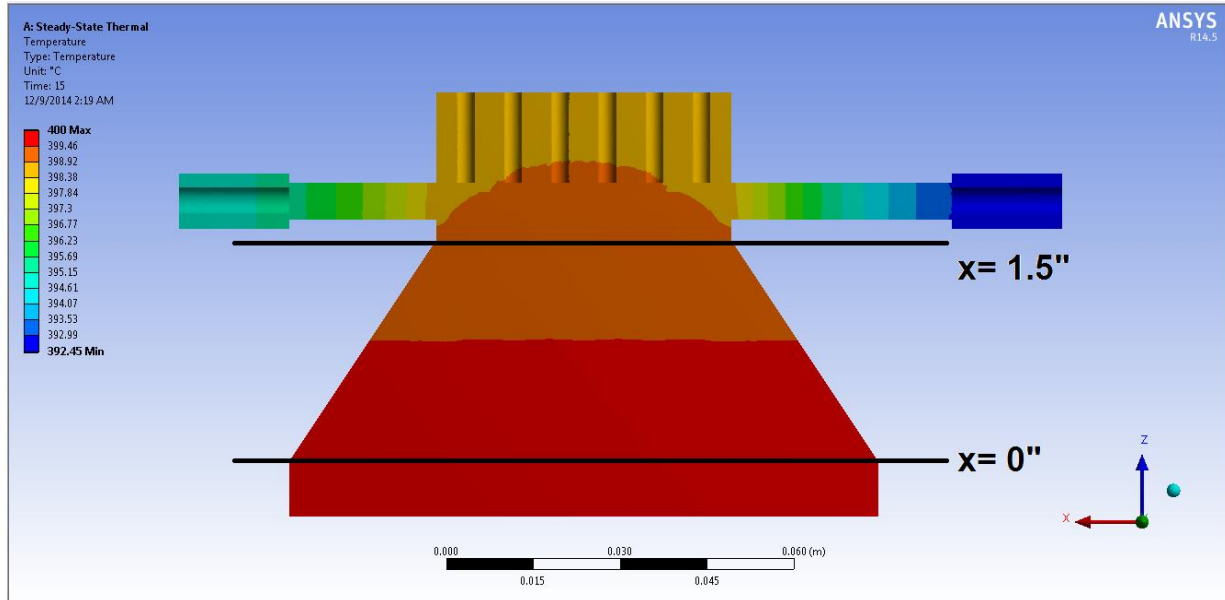


Figure 3. 14: Temperature profile for a simulation with a constant heat flux boundary.

The thick lines drawn on the temperature profiles represent the x-location limits, at $x=0''$ and $x=1.5''$ (3.81 cm). For the controlled boundaries, the constant temperature was 400°C (752°F), while the constant heat flux was valued at 7200 W or 24,567 btu/hr. The delta temperature for the simulations was both around 13.5°F (7.5°C). From these results, it can be concluded that any change in temperature is evenly distributed along a flat plane and as long as the distance between the thermocouples are significant enough to get a usable delta temperature value for analysis.

3.2.3 Final Design

From the finite element analysis of the block, two x-locations were specified to get a delta temperature for heat analysis. The final locations for the added thermocouples can be seen in Figure 3.15. These distances, at $x=0.25''$ (0.635 cm) and $x=1.0''$ (2.54 cm), were selected to ensure a noticeable change in x that will allow for an effective temperature analysis. The upper

thermocouple is close enough to the top of the block to get a good idea of how the temperature flows into the test section, but far enough to allow the wave of heat, after contact with the penetrating thermocouple, to flatten across the area when entering the test section contact interface.

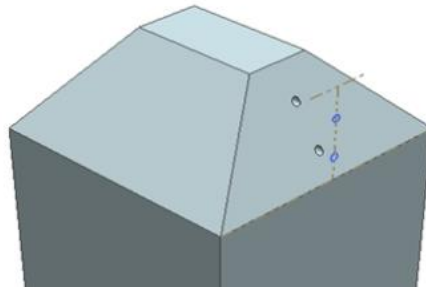


Figure 3. 15: Heating block with thermocouple penetration holes.

Probe-type thermocouples with a diameter of 1/8" were selected to penetrate the block. This size was selected because of thermocouple availability and ease of usage. Adding thermocouples required appropriate sized holes to be machined into the side of the block to secure the probes. The holes were made horizontal to the block to best measure the temperature of the block and minimize machining difficulty. To ensure that the temperature was accurately measured, the depth of these holes went as far as the centerline of the block. The holes were specifically made on the sides of the trapezoid that was not covered by the aluminum cradle to avoid any interference between components.

To observe whether the heat throughout the flat planes is even, shallow penetrating holes were placed at the same location on the opposite side to measure the surface temperature of the block, the depth of these holes were 0.0825" (0.21 cm) each. The CAD model of the block with the penetrating holes, showing their depth, can be seen in Figure 3.16.

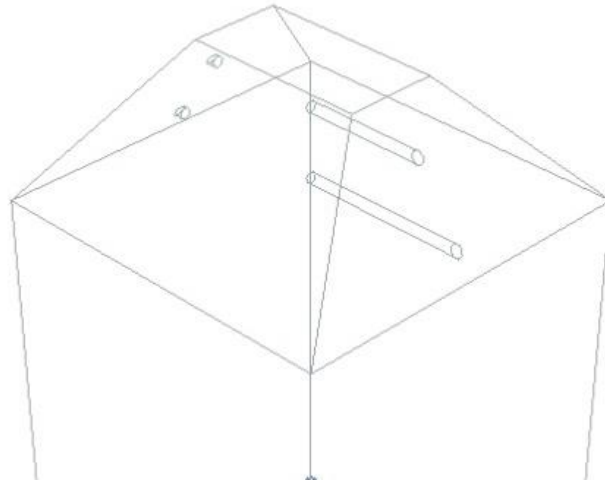


Figure 3. 16: Heating block with penetration hole depths.

The diagram in Figure 3.17 shows how the different thermocouples were arranged on the block assembly, inside the vacuum chamber. Probe thermocouples were used and excluding the inlet and outlet fluid temperature readings, the all thermocouples had an exposed junction at the tip of the probe. There are six TCs that read the fluid temperature along the heated channel to observe how the temperature changes with distance. These TC values were essential during the methane characterization tests to analyze this trend. In terms of this experiment, the fluid is water and is entering the channel at room temperature and much cooler than the heated block, E-type thermocouples are used. The inlet and outlet TCs use ungrounded E-type thermocouples to resist wear on the probe and accurately get the temperature of the fluid. A K-type thermocouple was added to the cradle to get the internal temperature for heat loss calculations in analysis. The added block thermocouples are four K-type thermocouples because of the high temperatures (similar to regenerative engines) the block is heated to. The last thermocouple measures the temperature of the vacuum chamber without contacting any component. It measures the empty space of the chamber to analyze how much the temperature rises.

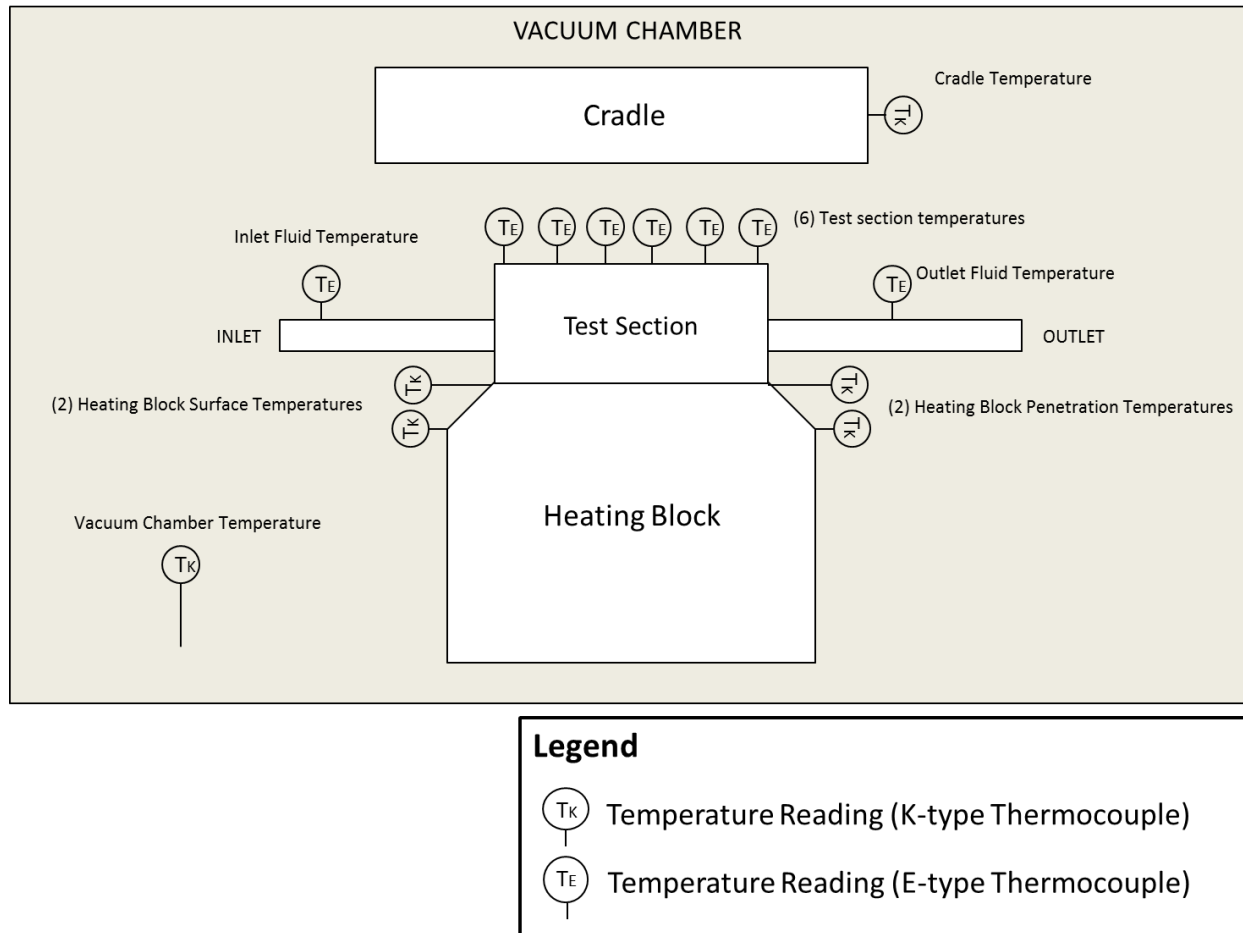


Figure 3. 17: Diagram showing the thermocouple locations that were used in the HHFTF.

The thermocouples were held in place inside the holes by securing them with a ceramic based paste called Resbond. The final heating block assembly with the attached thermocouples can be seen in Figure 3.18.



Figure 3. 18: Final heating block assembly with added thermocouples.

Chapter 4: System Integration and Components

The fully assembled experimental setup can be seen in Figure 4.1, below. The vacuum chamber that holds all the components of the HHFTF is made of 216-stainless steel and contains feed-through lines for the E and K-type thermocouples used inside. All the piping used in the assembly is composed of 316-stainless steel and has a 1/4" outer diameter. Swage compression fittings were used for all the connections, which include the connections to test channel, the line for the inlet and outlet, and all the valves connected to the setup. A detailed fluid schematic of the connections and components of the system can be seen in Figure 4.2.

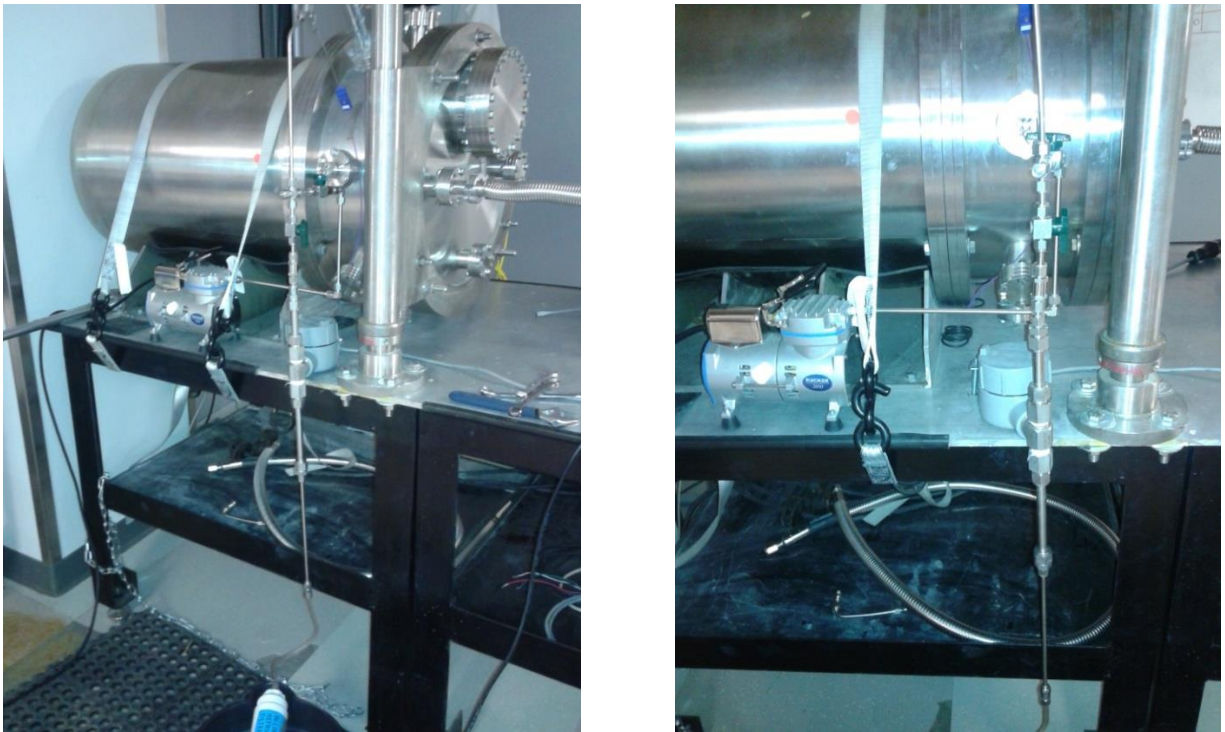


Figure 4. 1: Fully assembled HHFTF.

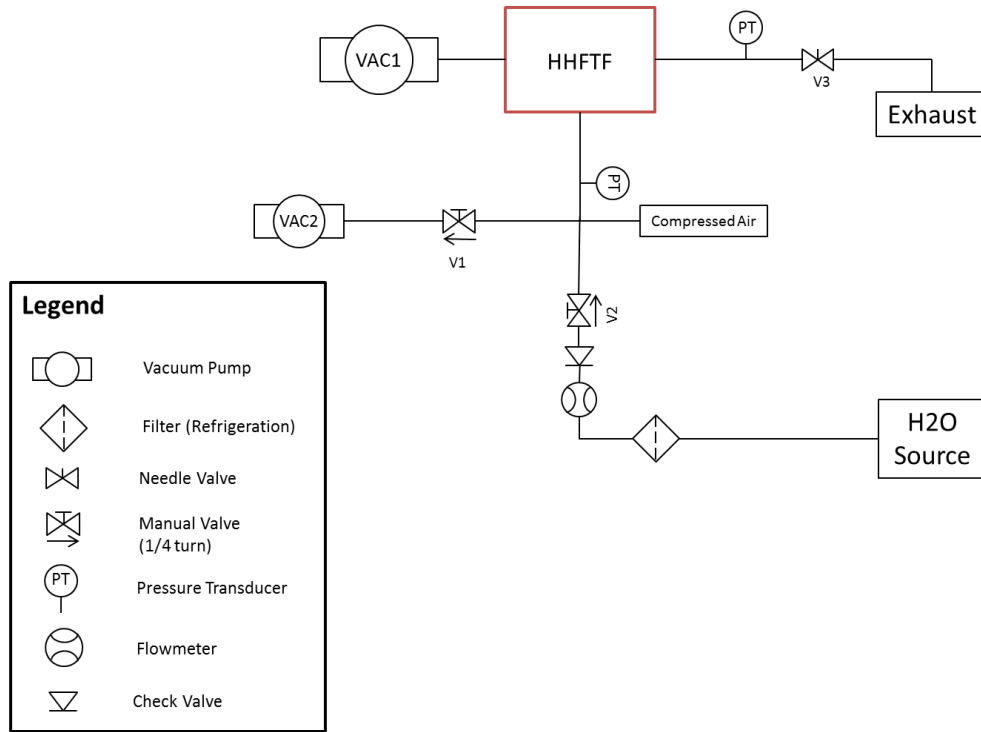


Figure 4. 2: Fluid schematic of the integrated system, including the HHFTF.

4.1 System measurements

4.1.1 Thermocouples

Thermocouples were used to measure the temperatures in the HHFTF. These sensors use two dissimilar metals that are connected at a junction and correlate temperature to a change in voltage. Two types of thermocouples were used for the HHFTF. The lower temperature readings used E-type thermocouples and the higher temperature readings used K-type thermocouples. Most of the thermocouples that were used had an exposed tip junction, due to quick response time, excluding the inlet and outlet fluid temperature readings, which were in direct contact with the fluid. A sheathed, ungrounded junction was used in those particular readings to avoid material degradation. The thermocouples were all probe thermocouples with quick-disconnect miniature connectors, as seen in Figure 4.3. The probes are made with

stainless steel and are fairly flexible. These thermocouple sensors were manufactured at OMEGA and were part of the MQSS series. The thermocouples had a 1/8" diameter of and the length of each probe was 6" (15.24 cm) long. Details regarding the thermocouples that were used can be seen in the detailed instrumentation list in the Appendix.

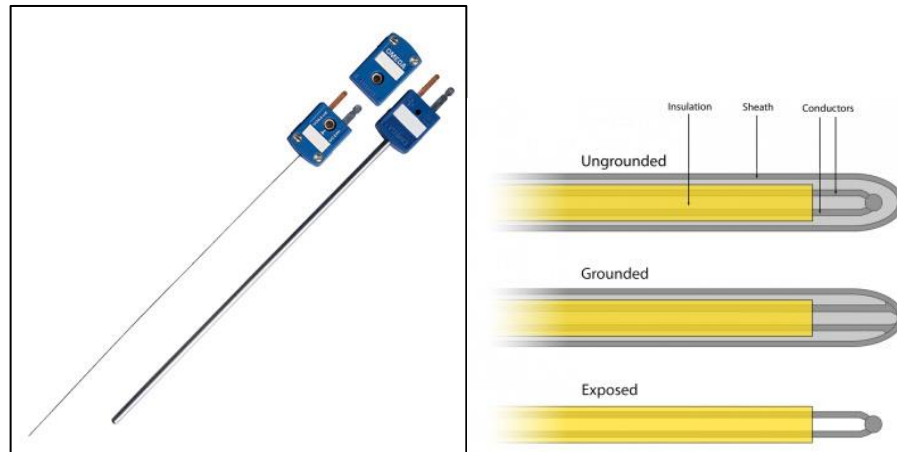


Figure 4. 3: MQSS Series Omega probe thermocouples used in the HHFTF.

4.1.2 Pressure transducers

The pressure of the fluid in the system was measured using pressure transducers (PT) that were manufactured by OMEGA. These PTs were PX1005L1-500AV Thin Film Cryogenic Pressure Transducers, as seen in Figure 4.4. Two PTs were used in different locations and each had a rating of 500 psi (3.45 MPa). One was placed at the inlet of fluid flow, and the other was placed at the outlet of flow, near the exhaust line. These pressure readings verified whether the flow and pressure drop between the inlet and outlet were consistent throughout a test. The pressure drop can also be used to correlate a mass flow rate of the fluid using Bernoulli's equation. The pressure transducers were connected to Omega Engineering DIN Process Meters, (Figure 4.4), and were calibrated to display a digital reading of the 'absolute pressure' present.

This was achieved by applying a measured change in voltage to a multiplying factor and displaying it as the correct pressure reading.



Figure 4. 4: The pressure transducer and process meter from OMEGA, used for system pressure readings.

A Kurt J. Lesker 317 Series Pirani Gauge was used with an MKS HPS 947 Convection Enhanced Pirani Gauge Controller to moderate the pressure levels inside the vacuum chamber. The gauge controller gave a clear reading of the real-time pressure value inside the chamber. Figure 4.5 shows the Pirani gauge and controller.



Figure 4. 5: Lesker Pirani Gauge for vacuum chamber pressure readings.

4.1.3 Flowmeter

To measure the fluid flow rate of the water going into the channel, a Hoffer Turbine flowmeter (HO Series) from Hoffer Flow Control, Inc. was used, as shown in Figure 4.6. This specific flowmeter was calibrated for water and made strictly for liquid flow. The flowmeter has a range between 0 and 17 L/min ($283 \text{ cm}^3/\text{s}$). Figure 4.6 also shows the transmitter used to export the flowmeter readings; it was also from Hoffer and of the C.A.T Series. The readings from the flowmeter came from changes in voltages that the computer program would change to gallons per minute. The flow rate was used to find the heat transfer rate in the data analysis. This transmitter has an excitation voltage between 13 and 30 volts and had to be connected to voltage-controlled device to operate effectively.



Figure 4. 6: Hoffer flowmeter and transmitter to get the flow rates of the fluid.

4.1.4 Data Acquisition (DAQ) and Graphical User Interface (GUI)

The HHFTF used a data acquisition (DAQ) system made by National Instruments (NI) which monitored the different system readings; this included the thermocouples, pressure transducers, and flowmeter. A DAQ system transmits a reading from a sensor to a computer program. For thermocouple readings, a NI 9213 16-Channel thermocouple input module was connected, via USB, to the experimental setup's main computer. The pressure transducers and the DC transmitter for the flowmeter were connected to the NI PCI-6533. The pressure transducers went through additional signal conditioning with a SCC-68 unit from NI. The digital components that were used for data processing are shown in Figure 4.7.



Figure 4. 7: Left to Right, a NI PCI-6533, a NI SCC-68, and a NI 9213 model.

Using the computer program LabVIEW 13.0 from National Instruments, the different sensor readings for the DAQ were calibrated and displayed on a graphical user interface (GUI). The GUI displays real time digital readings of temperature, pressure and flow rate. An image of the GUI used for this experiment can be seen in Figure 4.8. This file is called 'Water Calorimeter 2014' and is found on the desktop of the setup's main computer. The output of recorded data is in an LVM format and is automatically saved to a folder on the desktop called 'Water Calorimeter Data 2014'. To activate data recording, the switch graphic labeled as

‘Record On’ was used. As seen in the GUI, the charts on the right side display the specified temperature readings with respect to time. The block diagram that controls display in the GUI can be found in the Appendix (A1).

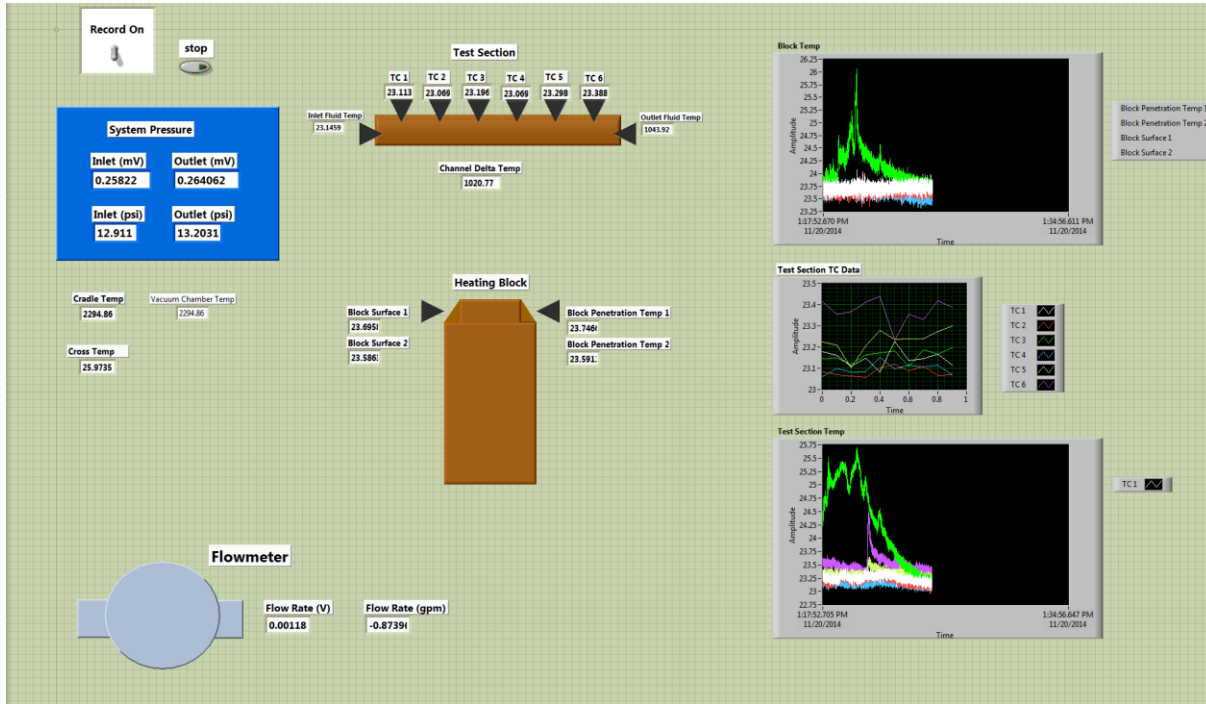


Figure 4. 8: Image of the GUI used for the HHFTF.

4.2 Valves

Several different types of valves were used in the HHFTF including Swagelok quarter turn valves, cryo-rated needle valves and check valves. Some of the valves used were rated for cryogenic flow because the liquid methane tests were incorporated into the HHFTF design. For this experiment, however, the fluid used was water and extremely low temperatures are not used in the line. All the connections for all the valves had an outer diameter of 1/4”.

4.2.1 Quarter-turn Manual Valves

Two quarter turn valves from Swagelok, as seen in Figure 4.9, were used for the piping in the system and are each rated at a max pressure of 1000 psi (6.9 MPa). One valve was used to

control the flow of water into the HHFTF, and the other was used to control the vacuum flow of the Rocker 300 vacuum pump. The valve design makes it easy to determine the direction of flow.



Figure 4. 9: Quarter-turn valves used from Swagelok.

4.2.2 Needle valve

To control the exhaust pressure, a cryo-rated needle valve made by Dragon Valves Inc. was installed at the outlet of the HHFTF. This valve can handle a pressure up to 9990 psi (68.9 MPa) and temperatures as low as -369 °F (-223 °C). Figure 4.10 shows the needle valve that was used.



Figure 4. 10: Needle valve from Dragon Valves Inc.

4.2.3 Check valve

As seen in the overall assembly, the flowmeter is placed upright and the flow of water goes up into it. The flowmeter uses a turbine that is designed for a single directional flow. To prevent any water from moving backward into the turbine, a poppet type cryogenic check valve was placed between the flowmeter and the quarter turn valve. This check valve was a SS-4C-5 Swagelok valve, seen in Figure 4.11, and has an allowable working pressure of up to 5 psi (34.47 KPa). The placement of the piping assembly can be seen in Figure 4.12.



Figure 4. 11: Swagelok check valve.

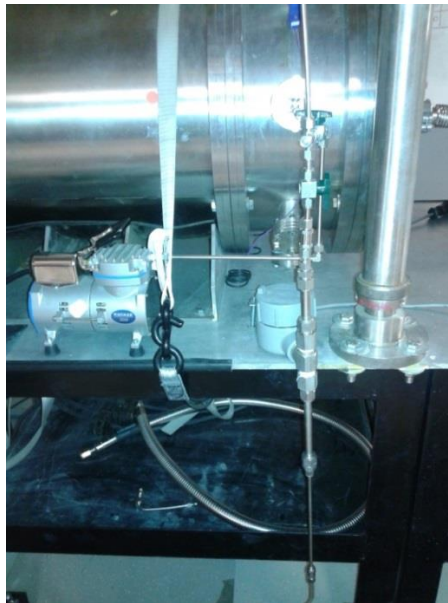


Figure 4. 12: Photo of the fluid piping system.

4.2.4 Water Filter

Potable water is available in the cSETR lab through a main-line pipe connection. However, there may be dirt and other deposit in the supply. For this reason, an in-line refrigerator filter from EcoPure, as seen in Figure 4.13, was attached to the test section's inlet supply. This filter would remove any dirt or unwanted minerals and give better credibility to the data results based on the known properties of water. The filter included 1/4" diameter hose with one end attaching to the water supply, and the opposite end connecting to the HHFTF via a 1/4" female swage connection.



Figure 4. 13: EcoPure in-line Refrigeration Filter.

4.3 Vacuum pumps

There were two different types of vacuum pumps used for the HHFTF. One was strictly used to pull vacuum inside the lines and another was used to pull vacuum inside the vacuum chamber, where the heating block assembly was located.

The Rocker 300 Vacuum Pump, manufactured by Rocker Scientific Co., Ltd. was selected as the pump to pull vacuum inside the lines of the HHFTF. This is a piston pump that uses a maximum power of 65 watts, and a max current of 0.7 amps; the maximum vacuum level was 0.11 Torr, at 2 L/min. Using 13 psi (89.6 KPa) as ambient pressure levels, this pump is able to pull vacuum down to 2 to 3 psi inside the lines. This pump also has a filter inside the inlet that catches moisture to avoid mechanical failure. The connection is a 1/4" swage connection that

easily attaches to the rest of the setup. The Rocker 300 pump can be seen in Figure 4.14.

Pulling vacuum in the lines is essential to the experimental procedure so that there is no excess residue inside the lines that may cause oxidation in the channel. Air expands at higher temperatures and leaving air in the lines during the heating process can cause undesired convective effects and affect the temperature readings of the thermocouples.



Figure 4. 14: Rocker 300 Vacuum Pump.

The BOC Edwards XDS5 Scroll Vacuum Pump, seen in Figure 4.15, was used to pull vacuum inside the vacuum chamber. This pump is capable of reaching an ultimate vacuum level of 4.5×10^{-2} Torr at 111.7 L/min. The placement of this vacuum in the HHFTF can be seen in Figure 4.16.



Figure 4. 15: BOC Edwards XDS5 Scroll Vacuum Pump.

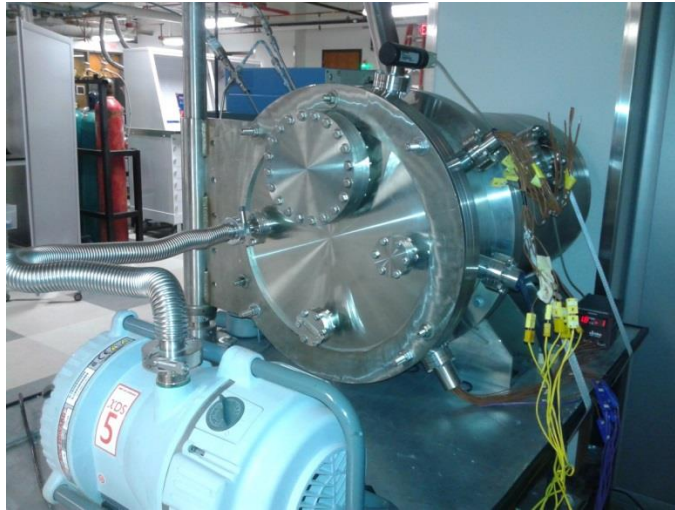


Figure 4. 16: Placement of Scroll vacuum pump in the HHFTF.

4.4 Electrical Components

There were three types of electrical sensor measurements that were critical to the HHFTF; this included pressure, temperature, and flow rate measurements. The main use of power in the HHFTF is the heating cartridges that are used to heat the copper block.

4.4.1 Heating Cartridges

Cylindrical cartridge heaters, which were manufactured at Gordo Sales, Inc., were used inside the copper block to provide heat to the test article. The heaters are 1/4" diameter tubes that are 5" long and at 120 volts, they each have a power rating of 400 Watts. An image of these heaters can be seen in Figure 4.17. These are resistive heaters that convert energy into heat by running a current through the tube and therefore, reach high temperatures very quickly. During an experimental test, if the heaters are on too long, the high current going through the heater will cause the coil inside to overheat and burn out the cartridge. To avoid this, the power sent to the heaters was manually controlled through a toggle switch by the test operator.



Figure 4. 17: Resistive cartridge heaters from Gordo Sales Inc.

A total of 18 heaters were used for the HHFTF due to available resources; the diagram in Figure 4.18 specifies how the cartridges arranged within the block. Since the heaters do not have support when the block is upright, a ceramic-based, high temperature paste called Resbond, was used to secure them inside the holes. This can be seen in Figure 4.19.

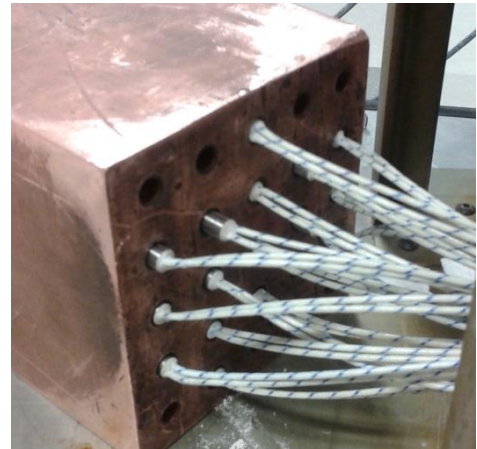
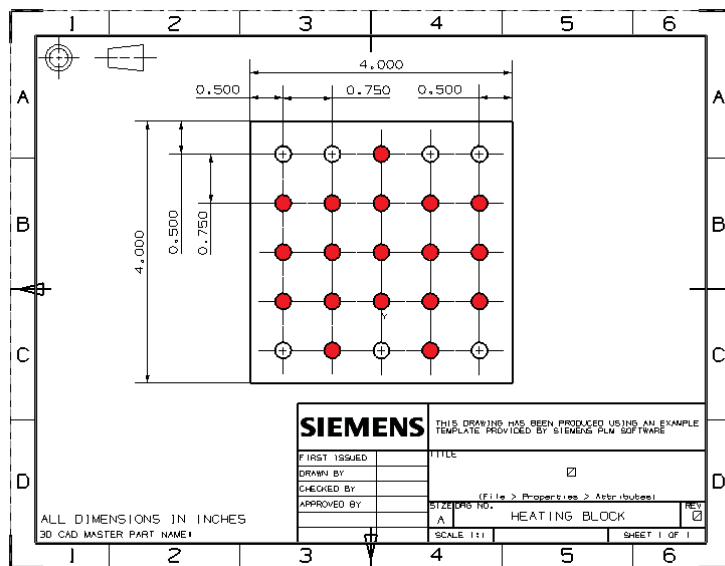


Figure 4. 18: Arrangement of cartridge heaters inside the copper block.

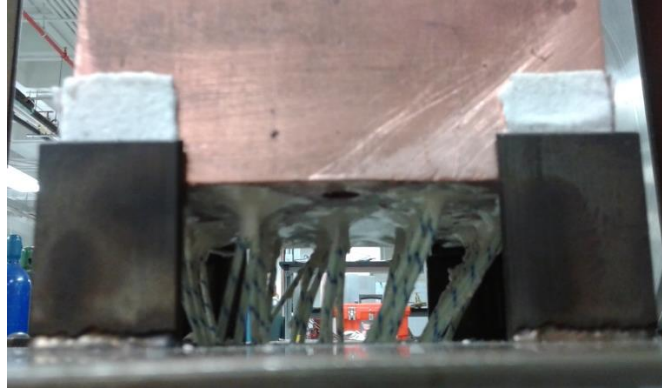


Figure 4. 19: Cartridge heaters secured with Resbond.

4.4.2 Solid state relays

Solid state relays (SSR) that are manufactured by OMEGA, used to control the cartridge heaters and are shown in Figure 4.20. To ensure that sufficient power is applied to each cartridge, three heaters were wired to each SSR, making a total of six SSRs used in the whole system. The solid state relays are rated at a maximum current of 50 amps and the resistance across each group of cartridges was measured to be ~12 ohms (36 ohms individually, wired in parallel). The SSRs were wired to NEMA-5 connectors available in the cSETR lab, for external power, and a manually operated toggle switch to control the heaters, also in Figure 4.20. The switch operated at 5 volts and therefore needed to be connected to voltage-controlled device. A max of 20 amps per NEMA socket is available at the cSETR laboratory is and using the SSRs ensured that the distribution of power would be adequate. A detailed wiring schematic of the SSRs can be found in the Appendix (A2).

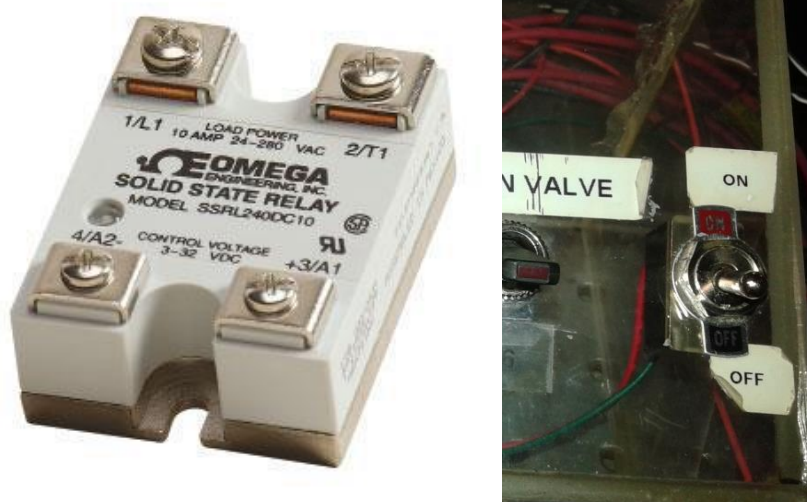


Figure 4. 20: Solid state relay used (left) and the switch used to control the power (right).

4.4.3 External Voltage Controller

DC-power voltage supply boxes were used to maintain the appropriate value of specific voltage and current levels required by electrical components. An Extech Quad Output DC power supply was used and can be seen in Figure 4.21. These boxes were connected to standard NEMA-5 power outlets and can be used to adjust the voltage and current levels that are required. The components that require the voltage from this power supply include the flowmeter, the pressure transducers, and the switch for the SSRs.



Figure 4. 21: Extech Quad output DC power supply.

Chapter 5: Methodology

5.1 Water Calorimetry

Calorimetry is an experimental method that measures the amount of energy that is being transferred within a system as heat. The science of this method was developed in the late 18th century and has a very wide range of applications. The word is derived from the Latin root ‘calor’, meaning heat, and ‘metry’ from Greek which means to measure [12]. To accurately measure this heat transfer process, calorimetry requires measurement of both the exothermic reaction of an object giving off heat and an endothermic reaction of another part absorbing heat. In the case of a heated channel, heat is absorbed by the fluid as it moves through and is, therefore, an endothermic reaction. The HHFTF’s primary focus is heat analysis through changes in fluid temperature so using a water calorimeter method for the system is a practical approach. The change in temperature as the fluid goes in and out of the channel can be used to analyze how much heat is transferred in the system.

Cryogenic fluids, like liquid methane, are prone to be two-phased during travel along a heated channel. However, to determine the heat flow values between the components in the facility, a water calorimeter analysis method was applied to the HHFTF. Water is a chemical that is well understood and fairly stable at a wide range of temperatures. The physical and chemical properties make it a liquid that can be used as a calibration fluid for a heat calorimeter method. In the HHFTF, the heating method used for a methane test was simulated and water was run through the channel, as methane would. An evaluation of the system was made by observing how much heat was absorbed at specified block temperatures (15). Various temperature and pressures readings throughout the HHFTF were used to determine the heat transfer of the system. A more detailed test procedure is described in section 5.3.

5.2 HHFTF Heat Transfer Model

The data collected from water calorimetry tests was analyzed for heat characteristics by using two approaches of numerical analysis. One approach uses conduction analysis by taking into account the vertical transfer of heat from the heating cartridges to the test section. The other approach is a convection analysis of the fluid travelling through the channel horizontally. The diagram in Figure 5.1 illustrates the two different heat transfer methods that were applied. The calculated heat values will be correlated to each other for further analysis.

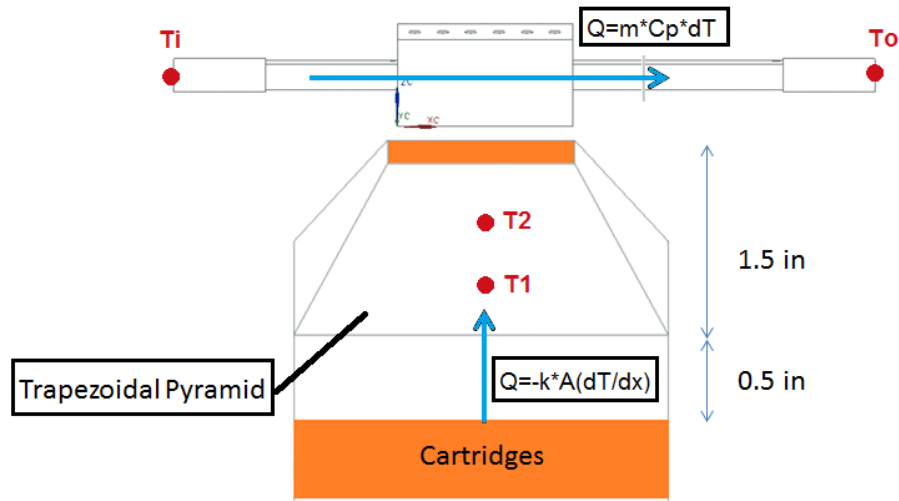


Figure 5. 1: Summary of Heat Transfer Analyses completed.

5.2.1 Convection Heat Transfer

To evaluate the heat transferred from the heated channel into the fluid, a convection relationship can be used. The general heat transfer equation, as seen below, Eq. (5.1), was the equation used for this fluid analysis [11].

$$Q_{\text{conv}} = Q = \dot{m} * c_p * \Delta T$$

(5.1)

Here, \dot{m} is the mass flow rate of the fluid, which in this case is water. Mass flow rate of the water was measured in the experimental setup with a turbine flowmeter at the inlet of the piping. The specific heat of the fluid, at a constant pressure, is presented as c_p ; this value was found using the known properties of water. ΔT is the change in the fluid temperature at the inlet and outlet of the channel. These are recorded with thermocouples that are in contact with the fluid but placed far enough from the channel inlet to affect the flow pattern. The Q value, in Watts (Btu/hr), can be found as the heat transfer rate from the channel into the water.

The parameters are derived from the fluid properties and allow the heat transfer rate to be found regardless of the fluid running through the channel. However, the Q value can change for different channel geometries and this should be considered for each analysis.

5.2.2 Conduction Heat Transfer

Since the HHFTF operates in vacuum and is insulated from metal-metal contact, the heat being transferred through the heating block can be seen as a one-dimensional, vertical heat analysis. The trapezoidal portion has a known geometry that follows a linear change in area as the vertical distance changes. Figure 5.2 illustrates this idea; by using distance A and B as the components of area, a linear equation of change in area in terms of x (vertical) can be found for any specified geometry [10].

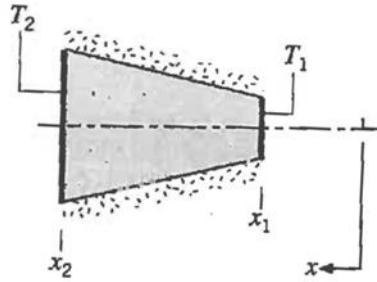


Figure 5. 3: Boundaries for 1-D conduction dependent on geometry [10].

Since the square prism portion of the block is heated with the cartridges, analysis for this method begins the x -distance at the trapezoidal portion, which is a height of 1.5". Based on the heating block geometry, an equation was found for the changing rate of area based on the vertical change in distance, $A(x)$. Using this equation, the heat transfer equation for variable area was found and used in analysis. As mentioned earlier, Q is dependent on temperature and distance so the temperature readings from the thermocouples that penetrate the wall are plugged into the Q equation to be analyzed. Figure 5.4 shows the labeled axes of the analysis and the location of the thermocouples. For the sake of analysis, the values used for these calculations were solved in English units and converted afterwards to metric for required data comparisons.

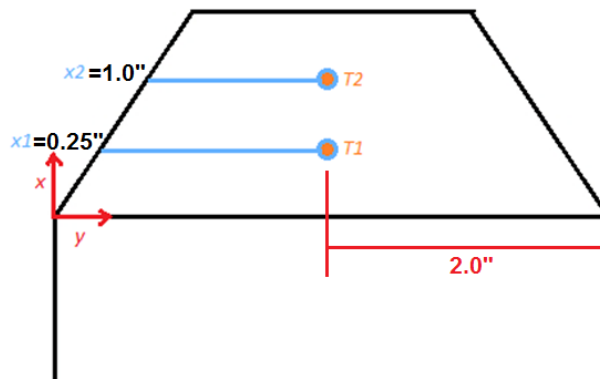


Figure 5. 4: Illustration of the boundaries in the model.

5.3 Experimental Procedure

The overall test procedure can be summarized as conductively heating a copper block that directs heat to a single channel test section. Water flows through the test section and thermocouple readings placed throughout the block assembly measure how the block and test section responds during a test. To accomplish this task, the experimental procedure can be separated into three main categories: the pre-testing procedure, water flow testing, and the post-test procedure. A full step-by-step procedure can be found in the Appendix (A4).

5.3.1 Pre-test Procedure

Because the HHFTF uses high power devices, it is important to inform others when a test will be conducted. Before a test is performed, continuity between all the thermocouples and the metal components must be established. Specifically, the thermocouple junctions on the copper block, cradle, and test section should all be in contact at the appropriate contact points.

Using a multi-meter on the continuity setting, the contact is checked by placing a probe between the metal portion of the TC's mini-connector and the other on the metal it should be in contact with. A beeping sound will be produced once a contact is created. It is very important to ensure this connection before testing to get accurate temperature readings from the thermocouples. After contact is confirmed, the vacuum chamber can be closed with the available 1/2" nuts and bolts that fit into the door of the chamber. When the chamber is closed, the XDSS vacuum is secured with an O-ring and metal clamp and is turned on to pull vacuum in the chamber. The chamber pressure is monitored with the Pirani gauge and controller. The power cords from the SSRs should be connected to six separate circuit NEMA-5 power outlets. Voltage across the SSRs must be checked to confirm that all the cartridge heaters are working

properly. By placing a multi-meter on the voltage setting, the voltage across the metal +/- connections should read 120 volts.

Afterwards, the hoses that are attached to the refrigeration filter need to be connected to the water source available in the cSETR lab. The tubing is connected and secured via a hose clamp to the water source and a 1/4" swage connection to the HHFTF on the other end. At the HHFTF outlet location, a small length of tubing is connected with a 1/4" swage connection to a water drain. At this point all the valves should be closed. The LabVIEW program on the computer titled 'Water Calorimeter 2014' must be opened and ran to check that the real time results are reading ambient conditions. The voltage box should be turned on, and the voltage current levels for the specific channels should be checked.

5.3.2 Water Flow Testing Procedure

The testing procedure can be described using a simplified version of the fluid schematic in Figure 5.5. When all the test preparations have been completed, V2 is opened along with V3 to allow the water to flow through. After the valves are open, the H₂O source is opened slowly to avoid overturning the turbine in the flowmeter. The flowmeter has a maximum voltage measurement of 5.0 volts and overturning it would render it unusable; this voltage can be monitored by the real time reading displayed in the GUI. As the water source is opened, the water flows through the HHFTF and into the water drain. The temperature of the test section is monitored for steady state flow.

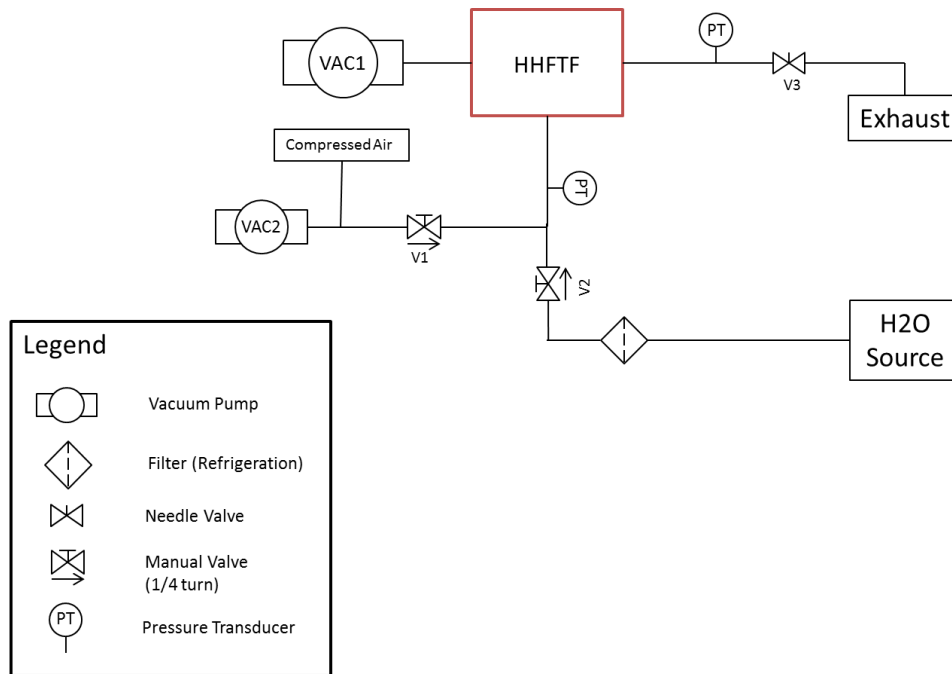


Figure 5. 5: Simplified Fluid Schematic of the HHFTF.

Using the controlled block temperatures that are specified in the experimental test matrix, the block is manually heated using the heater switch on the switchbox. A 3-second on and 3-second off toggle pattern is used to heat the block without overheating the heaters. The block temperature must be constantly monitored during heating to reach the exact temperature for the test. Water is flowing continuously through the block as it is heated to different temperatures. When the desired temperature is met, the GUI was observed to see that the water flow rate is fairly steady. When both these items have been checked, the data was recorded for a period of 30 seconds by selected the ‘Record On’ button on the GUI. The temperature of the block was kept at the desired temperature for the duration of the test by heating as necessary. Pressing this button again stops the data from recording. The block was then heated again to reach the next temperature in the test matrix. The same recording process was implemented until all the data points have been recorded.

5.3.3 Post-testing Procedure

When all the data has been collected, the water source and V2 was closed. The compressed air available in the lab was used to purge the water inside the line to avoid any residue from sticking inside the line and affecting the data of the next test. All the lines and hoses are purged with the air gun and connections were secured for a next test. The voltage box was turned off and the SSRs were unplugged. The XDSS Vacuum was left running for a few hours to ensure that the block cools down in vacuum; this was to avoid any oxidation from building between the metal contact points in the setup, especially between the block and the test section interface.

5.3.4 Additional Testing Method

An additional type of test was performed that followed a similar method but treated each data point as a full test. After each block temperature was reached, V2 and the water source valves were closed and the line between the test section and exhaust hose were purged with air. Vacuum was pulled in the lines with the Rocker 300 pump by opening V1 and closing V3; vacuum levels in the line went down to around 2-3 psi (13.8-20.7 KPa). The block was heated to the following temperature in complete vacuum. When the block reached the desired temperature, V1 was closed and V2 and V3 were opened along with the water source. The block was then treated as a decaying heat source to observe how the water would affect the block and test section temperatures. This method is similar to the process used during a liquid methane test and was used to analyze how the heat flux from this method would compare to tests with continuous water flow.

Chapter 6: Results and Analysis

6.1 Test Matrix Development

The test conditions that were selected were centered on the temperature of the heating block because it is the lone controlled variable in this experimental system. Other variables, such as system line pressure and flow rate were determined as a constant based on the available water pressure inside the lab. This pressure remained fairly constant at around 30 psi (207 KPa); the flow rate, based on flowmeter readings, remained around 0.027 L/s (0.0276 kg/s). The temperature of the heating block for each test point is specified in the test matrix in Table 6.1.

Table 6.1: Experimental Test Matrix for Water Calorimeter Test.

Block Temperature (°C)	Block Temperature (°F)	Duration (sec)
24 (room)	75.2	30
50	122	30
100	212	30
150	302	30
200	392	30
250	482	30
300	572	30
350	662	30
400	752	30

6.2 Heat Transfer Rate Calculations

As specified in section 5.2.1, there were two types of heat rate analyses that were performed. One method is a convection-based analysis, while the other is based on conduction.

6.2.1 Convection Analysis

The convection analysis, as described in section 5.2.1, used the averaged value of the steady fluid inlet and outlet temperatures to evaluate the heat transferred from the heated channel into the fluid. Each test point had the fluid temperatures to be averaged across time. The mass

flow rate was taken from the flowmeter reading and the specific heat, at constant pressure, for water was used as the constant value of 1 btu/(lb°F), or 4.18 J/(g° C).

6.2.2 Conduction Analysis

The conduction method used is described in section 5.2.2. Using Fourier's law of conduction, the equation for conduction, Eq. (6.1), can be extended into an integral to obtain the overall heat transfer rate through the entire geometry, Eq. (6.2) [10].

$$Q(x, T) = -k * A * \left(\frac{dT}{dx} \right) \quad (6.1)$$

$$\int_{x_1}^{x_2} \frac{Q(dx)}{A(x)} = \int_{T_{\text{block}}}^{T_{\text{top}}} -k(T) * (dT) \quad (6.2)$$

The value for thermal conductivity was used for pure copper varies slightly with temperature, but under the conditions used in this experiment, it is assumed as a constant. This analysis used a value of 19.25 Btu/(hr*in*F), or 401W/mK for conductivity. Based on the heating block geometry for the HHFTF, Eq. (6.3) was found to express the changing rate of area is dependent on the vertical change in distance. 'x' is the vertical distance between the bottom of the trapezoidal section and the test section contact interface. Figure 6.1 shows the labeled axes of the analysis and the location of the thermocouples, for clarification.

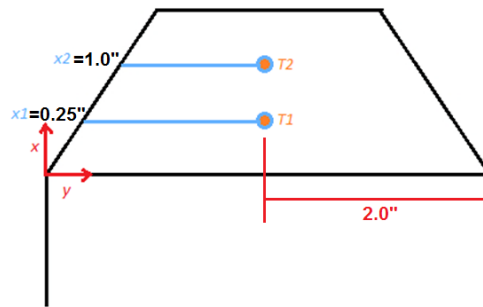


Figure 6. 1: Block with labeled axes used in conduction analysis.

$$A(x) = \frac{8}{3}x^2 - \frac{40}{3}x + 16 \quad (6.3)$$

The limits of the area equation can be described as $0 \leq x \leq 1.5$ in (0.0381 m). By substituting the $A(x)$ equation into the integral, Eq (6.2), and performing the integral, the Q -equation for the block was found to be equation Eq .(6.4). Eq. (6.5) shows the final heat transfer equation that is used for the heat transfer analysis.

$$\frac{Q}{4} * \ln \left(\frac{(x_1-2)*(x_2-3)}{(x_2-2)*(x_1-3)} \right) = -k * (T_2 - T_1) \quad (6.4)$$

$$Q = - \left(\frac{8}{3} \right) * \frac{k*(T_2-T_1)}{\ln \left(\frac{(x_1-2)*(x_2-3)}{(x_2-2)*(x_1-3)} \right)} \quad (6.5)$$

6.3 Data Analysis

The data recorded from each test included 14 temperature readings, a flowmeter reading, and 2 pressure readings. The GUI displayed in Figure 4.8 shows all these readings. The thermocouple readings included 6 test section skin temperatures, along the channel, an inlet and outlet fluid temperature, 4 heating block readings, a penetrating cradle temperature, and a vacuum temperature reading. The data from these thermocouples were recorded in degrees Celsius. The flowmeter used its transmitter to display the flow rate of the fluid in gal/min (GPM). The two pressure readings included the inlet and outlet pressures, read from the pressure transducers and the output was in psi. Two test trials were performed using the continuous flow method and one trial used the additional method of purging the lines after each test point. Although English and Metric units are mixed in the data collection, analysis used the proper units of conversion.

6.3.1 Continuous Water Flow Test

The experimental method to collect data used a continuous flow of water as the block was heated to the temperatures in the test matrix. When a point from the test matrix was tested, the flow was steady and recorded for a period of thirty seconds; this allowed the data to be easily averaged across time for each specified block temperature. The initial analysis of averaging the temperatures provided a chart that had a single value for each variable, at each temperature.

Figure 6.2 shows an example of the temperature readings for Test 1, plotted against block temperature.

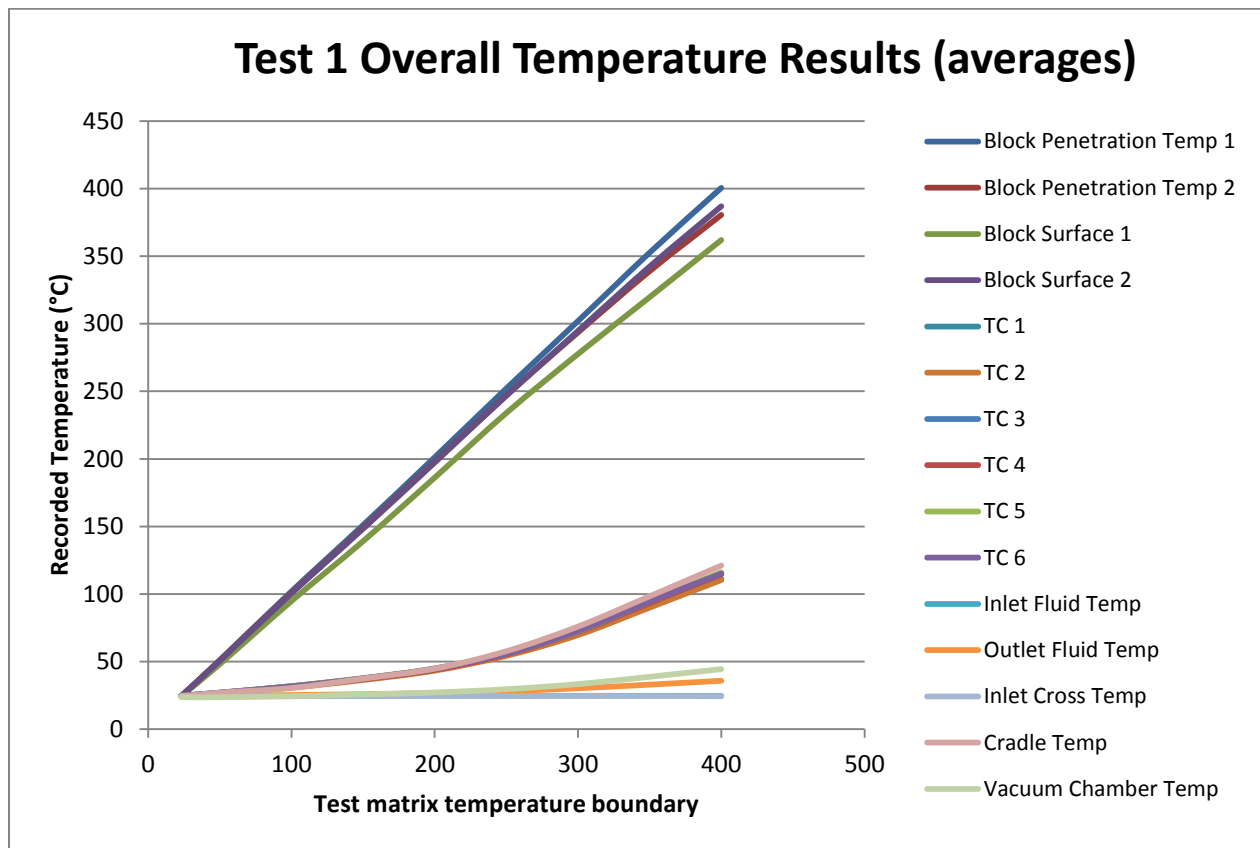


Figure 6. 2: Example of Overall Temperature Results with increasing Block Temperature.

After the initial analysis was complete, the readings were observed for various trends. The system's thermocouple results followed a predictable pattern as block temperature rose.

Between the four block temperatures, the delta temperature at the different x-locations was more significant at higher temperatures. As seen in Figure 6.3, all the block temperature readings were fairly similar except Block Surface 1, which was a much lower temperature through the test. This is an understandable trend because this thermocouple probe is fairly far from the center of the block. To ensure that the data best represent the overall temperature trends, the data recorded for Block Penetration Temp 1 and Block Penetration Temp 2 were used to get the conduction heat transfer rates. As expected, results from Test 1 and Test 2 yielded similar temperature ranges.

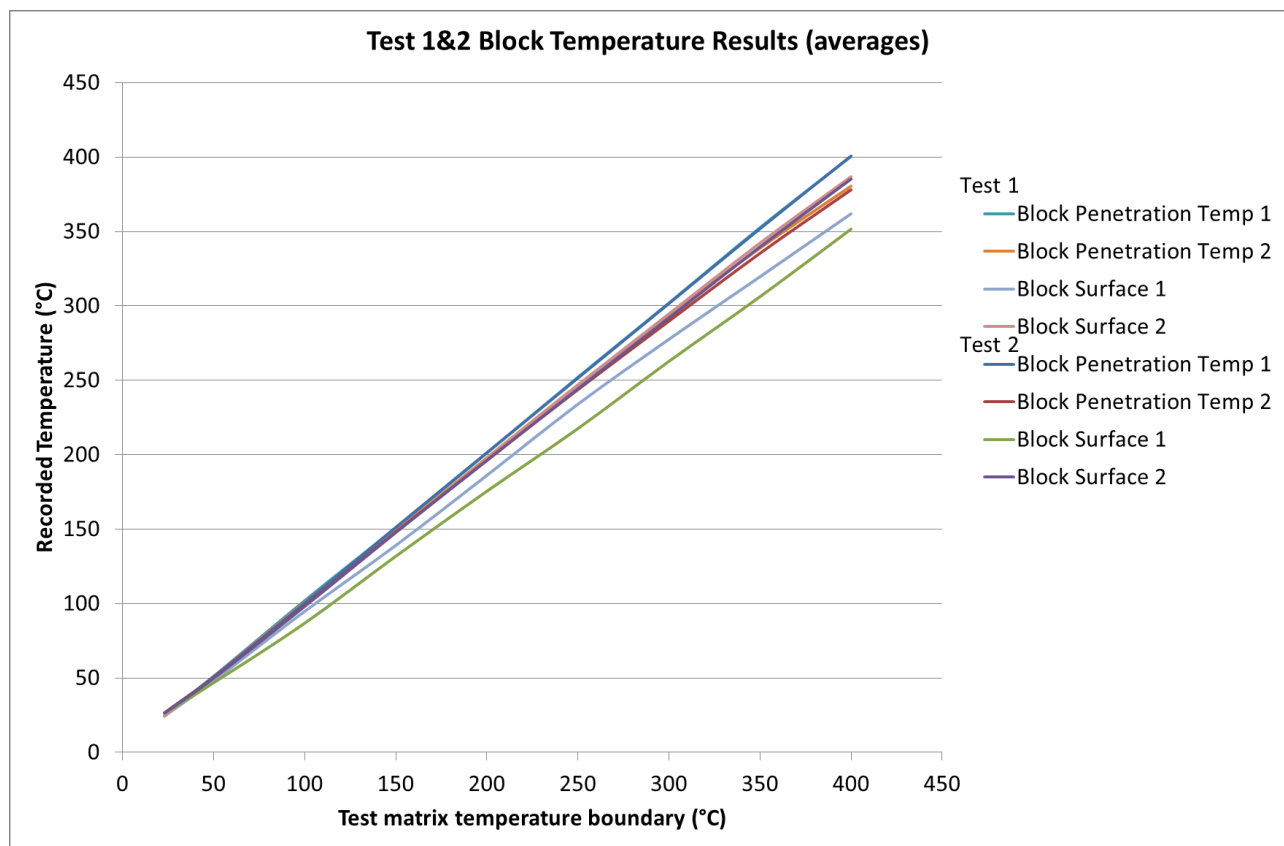


Figure 6. 3: Actual Block Temperature readings, as Temperature increases.

6.3.2 Stopping Water Flow Test

For the additional testing method, the line was purged of water after each test point and vacuum was pulled in the lines before the block was heated to the following block temperature. The block acted as a 'decaying heat source,' and yielded a plot that decreased over time and evened out to a steady temperature for each thermocouple in the system. An example plot of a single test point, temperature at 150°C, can be seen in Figure 6.4. Predictably, since vacuum is pulled in the lines, the block heats up much quicker and there is no heat lost during the heating process. This test method served two purposes including analyzing the trend of system temperatures when the block was heated in full vacuum and then exposed to a cool fluid and the heating characteristics of the block with no convection loss effects.

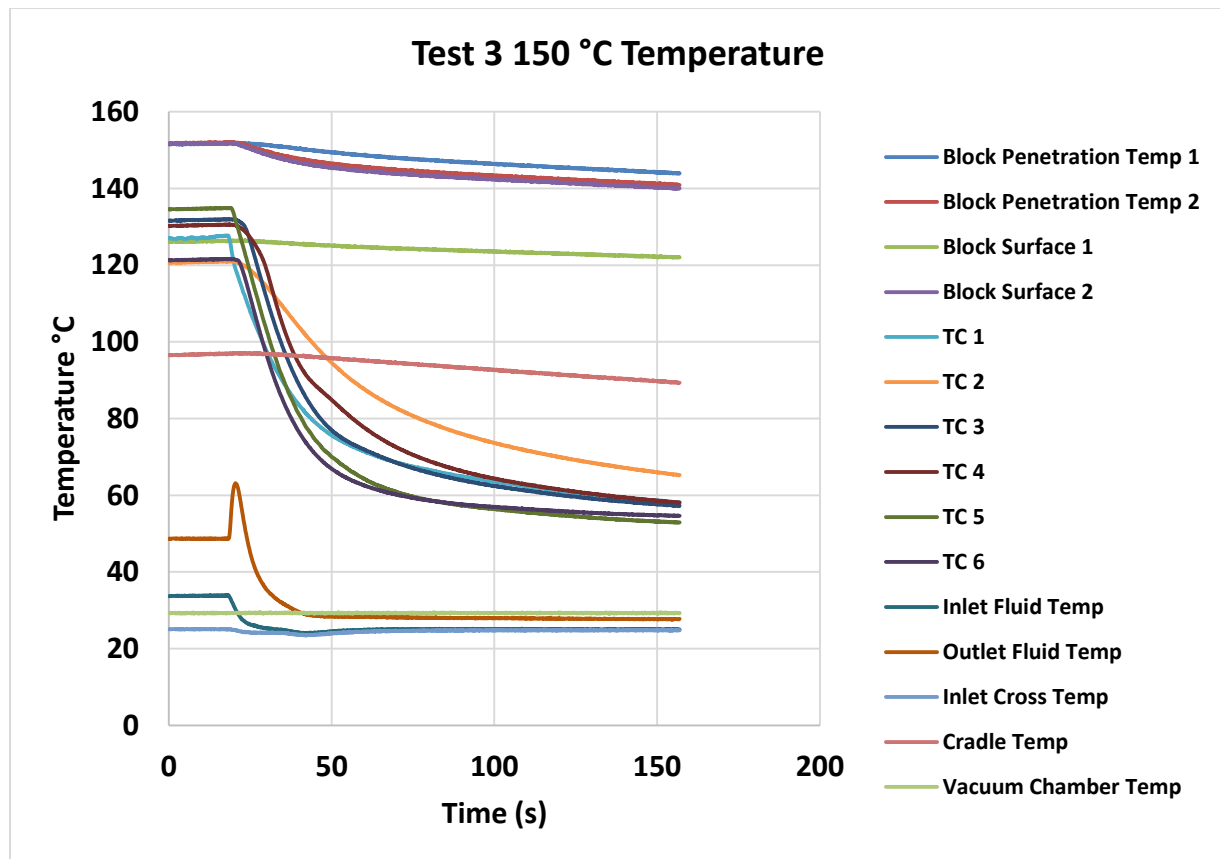


Figure 6. 4: Temperature results of Test 3 at 150°C.

The beginning portion, which can be described as a flat temperature cross the components, was used for loss analyses between the different HHFTF components; the ending portion can also be seen as a flat temperature for a period. Figure 6.5 shows an example of how the data for Test 3 was analyzed.

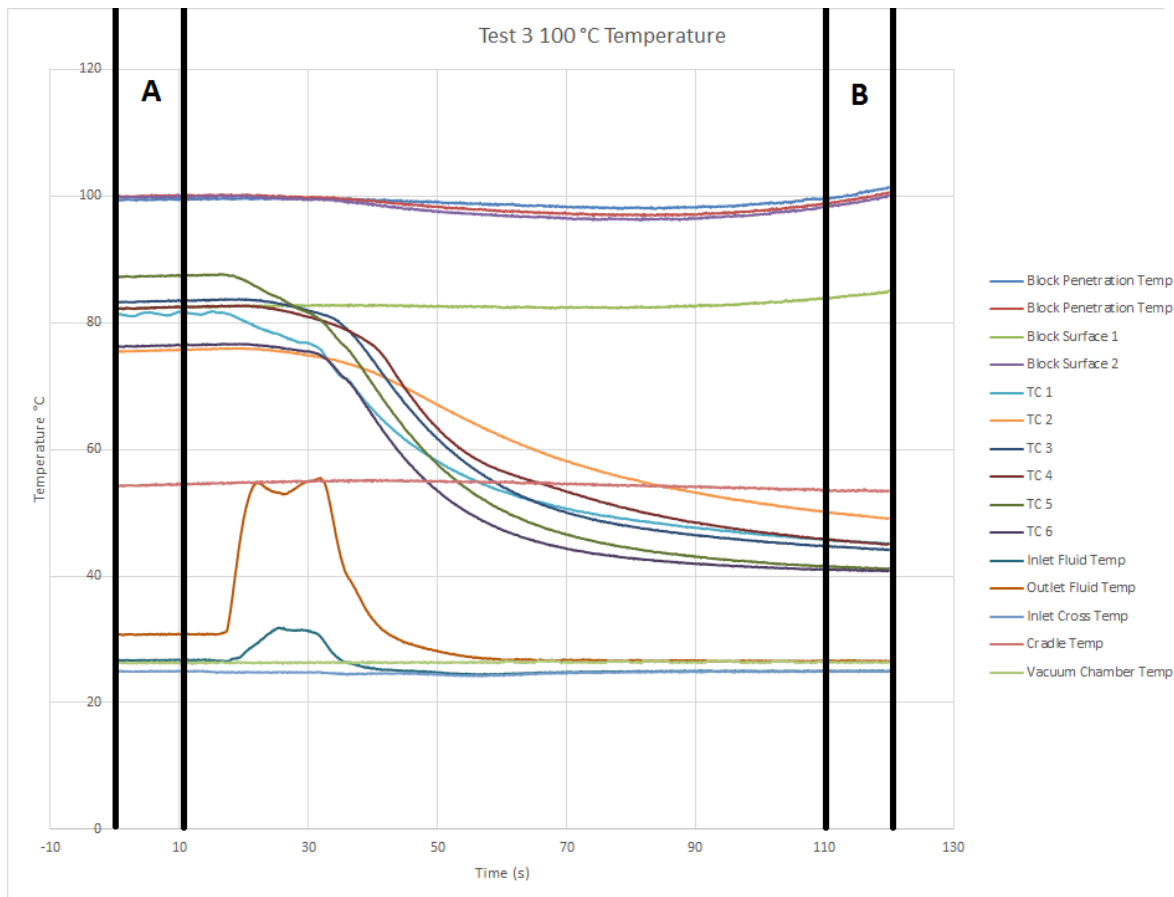


Figure 6. 5: Analysis approach for Test 3.

Section A was used to find the conduction losses of the system due to the cradle temperature. A 10 second increment of the cradle temperature was taken and averaged across time to get a single cradle temperature at each block temperature. A detailed analysis for Section A is found in section 6.5.

Section B is also a 10 second increment and was analyzed using a process similar to the method used in Tests 1 and 2. This portion was taken as a constant temperature and heat transfer rate was found.

6.4 Data comparisons

The data recorded from the tests was analyzed to find the heat transfer rate at each test point.

Both heat analyses were observed and the results from the tests can be found in the plots below.

6.4.1 Convection Analysis

Figure 6.6 summarizes the results for calculated heat transfer rate using the convection analysis method, from section 6.2.1. The results from each test are relatable and gave a definite positive trend as block temperature went up. The three tests yielded similar results that verify the repeatability of the test procedure. The range for convective heat transfer rate was between 26.9 and 1490 J/s (91.8 to 5084 btu/hr).

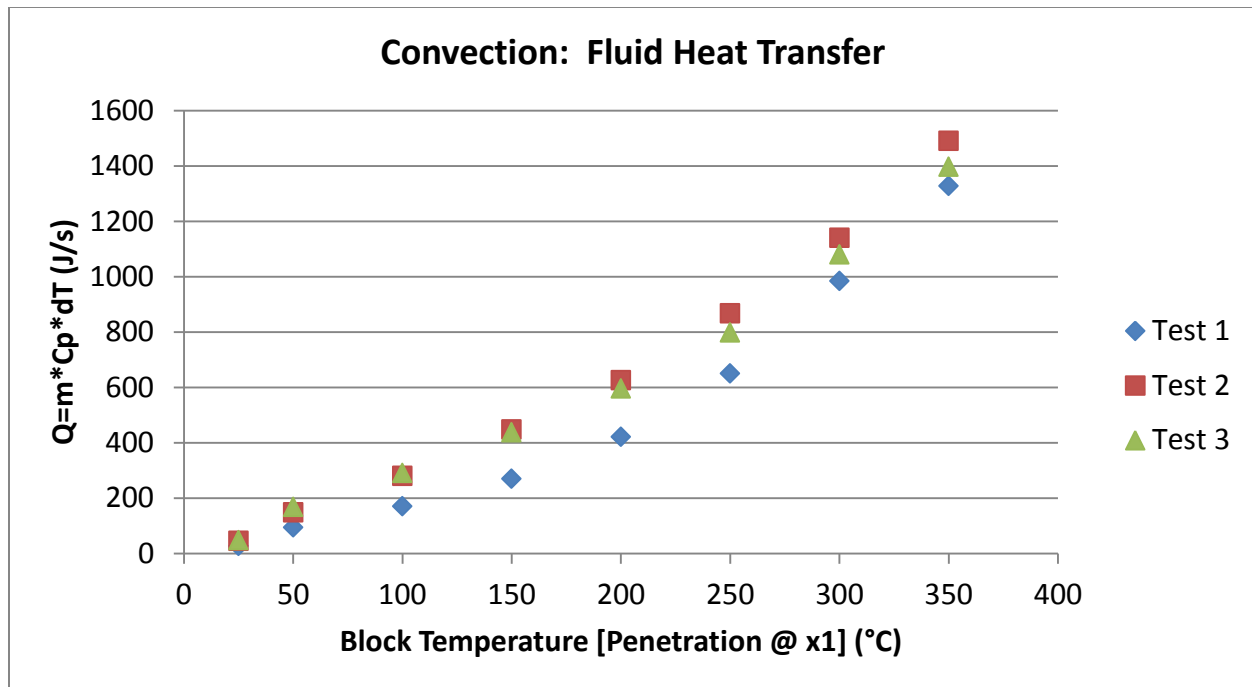


Figure 6. 6: Convective Heat Transfer Results.

6.4.2 Conduction Analysis

Figure 6.7, below shows a plot of the heat transfer values that were calculated for each test using the conduction equation found in section 6.2.2. The results follow a similar trend to the convective heat results, but at much higher values. The range for the conductive analysis is between 79 and 5872 J/s (269.6 to 20,036 btu/hr).

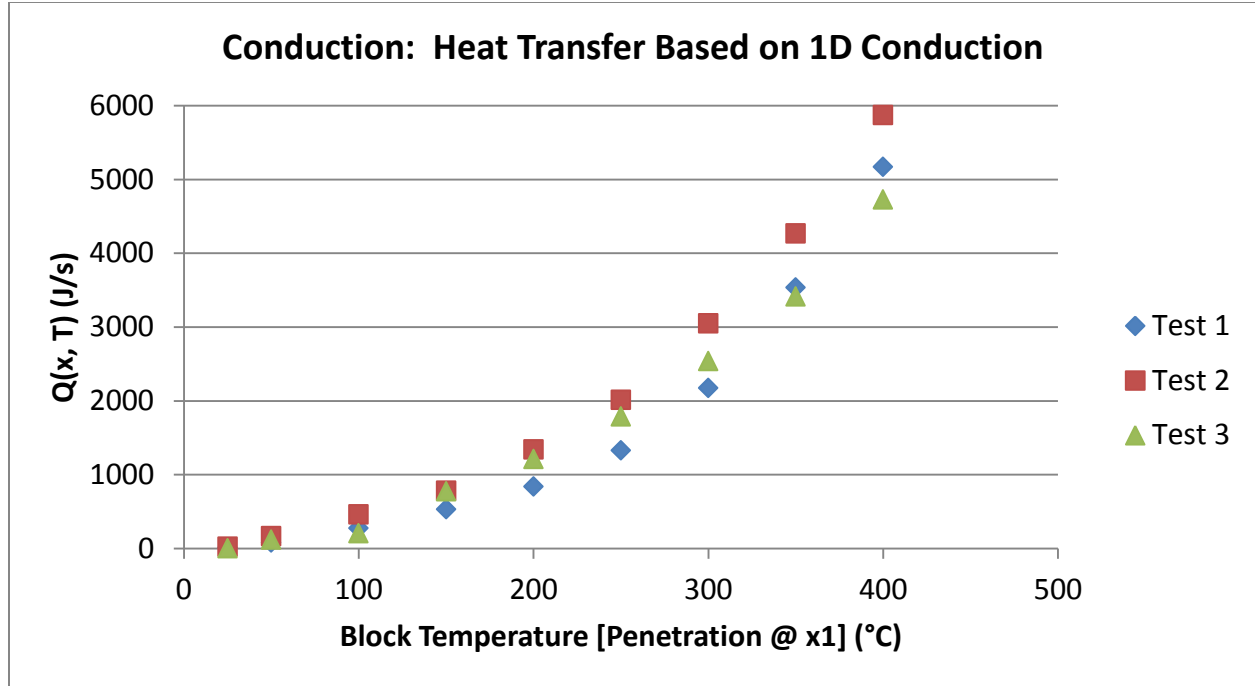


Figure 6. 7: Conductive Heat Transfer Results.

6.4.3 Heat Transfer Correlations

Theoretically, the heat being transferred through the block via conduction and the heat moving into the fluid through convection should be relatable. To correlate the results from two different methods, a ratio was plotted of the multiplying factor between the values. The results show the variation between these two heat transfer measurements. Eq. 6.6 was used as the ratio of heat transfer to compare the data. As seen in the previous plots, the heat transfer value for the conduction analysis is much greater and was, therefore, arranged get a multiplying factor.

$$Q_Ratio = \frac{Q_{penetration\ TCS}}{Q_{m \cdot Cp \cdot dT}} \quad (6.6)$$

Figure 6.8 shows a plot of this Q_Ratio with respect to the temperature difference between the penetrating thermocouples. This delta temperature was used because it best represents the change between the locations regardless of the block temperature. As seen here, the conductive

heat transfer, was roughly 3.1 times greater than that of the fluid heat transfer. The plot in Figure 6.8 supports this observation.

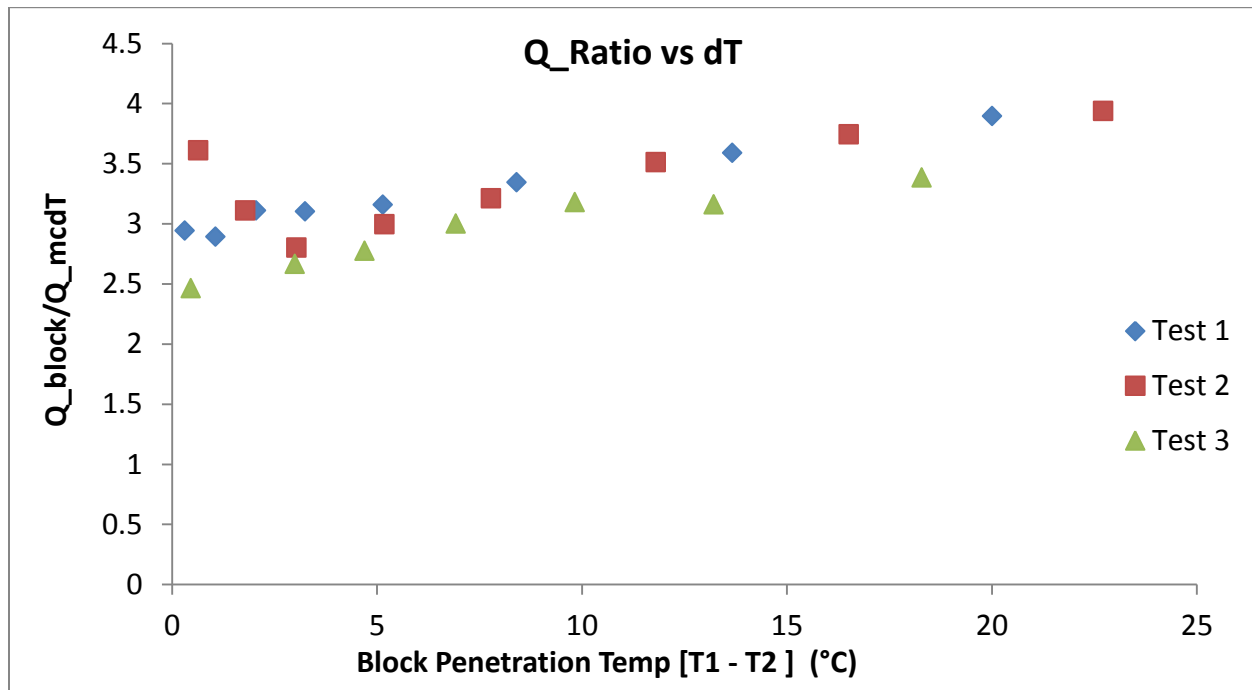


Figure 6. 8: Conduction and Convection Heat Transfer comparison.

Unfortunately, this result shows that there are considerable heat losses between the heat going into the block and into the channel fluid. However, because of the consistency of the results, as seen in Figure 6.9, the correction factor between these two heat values remains at a fairly constant value at 3.1. Figure 6.9 correlates the Q_Ratio for all the results as a single trendline; the trend is linear and slope for these values is very low at 0.044.

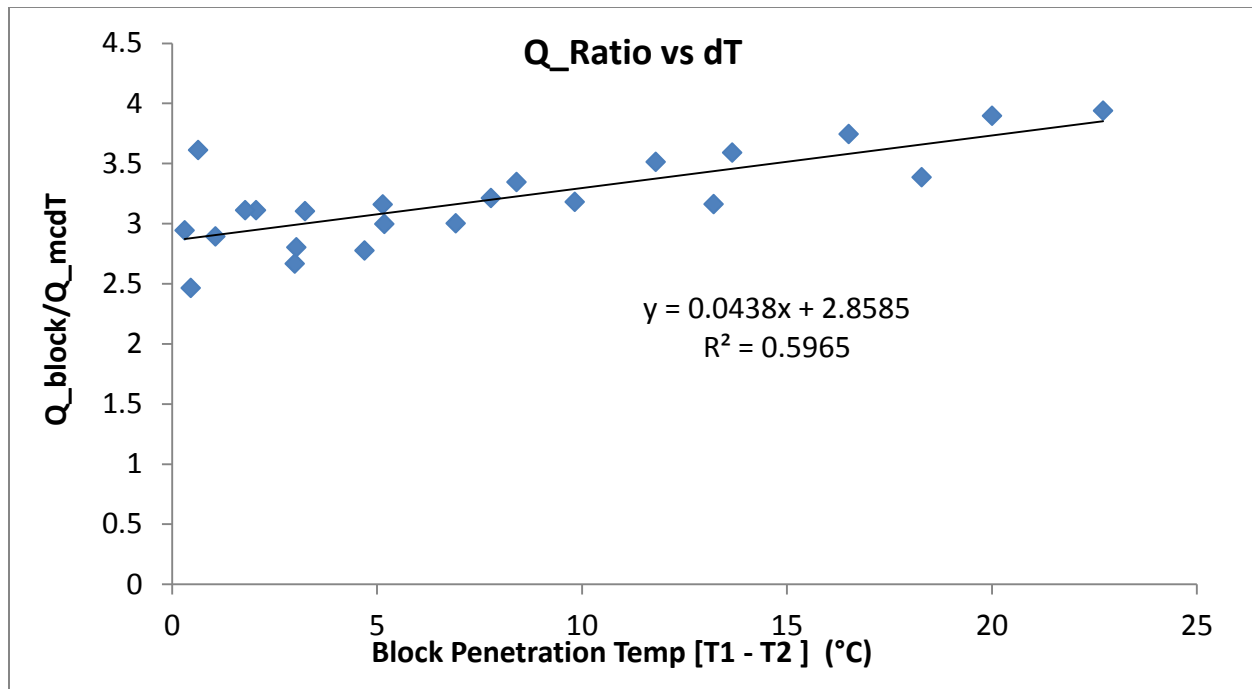


Figure 6. 9: Trendline of all Q_Ratio values found.

Figure 6.10 shows the overall trend of how the convection-based Q-value varies in relation to the delta temperature, by plotting the values against the delta temperature of the block thermocouples. By plotting the convective Q values, against the delta temperature, a relationship can be found between the two heat analyses. The results from all the tests are plotted below.

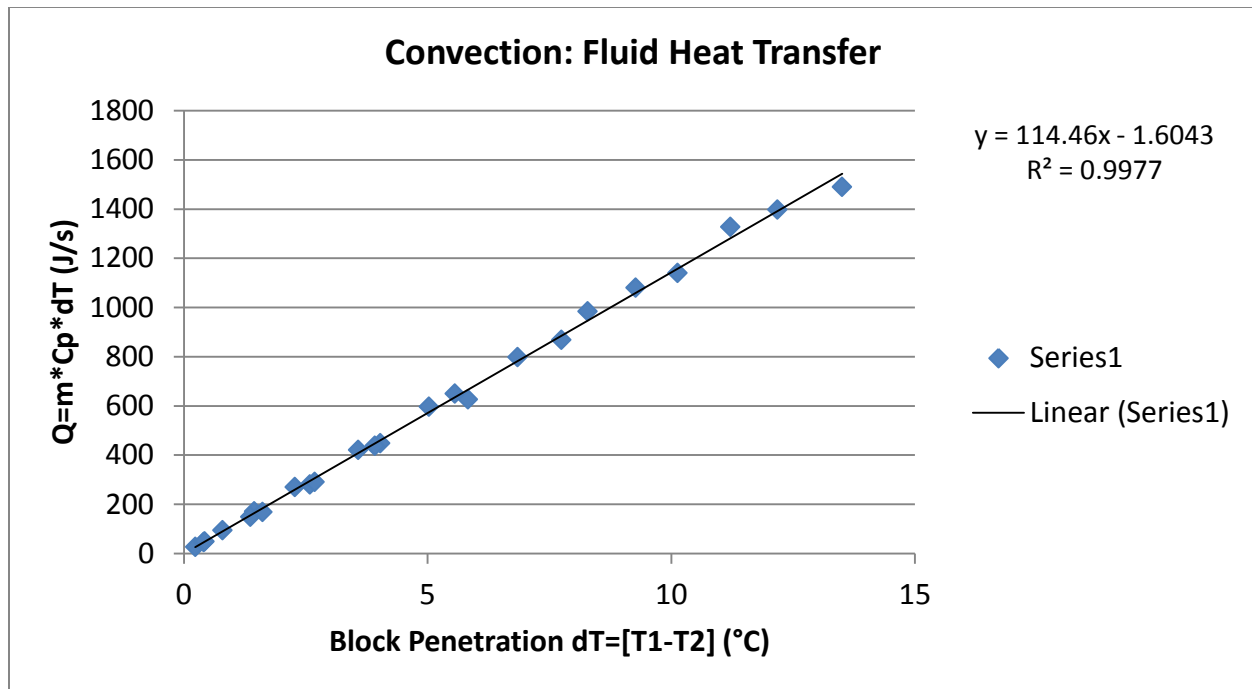


Figure 6. 10: $Q_{\text{convection}}$ vs. dT of Block.

This plot can be used as the relation between how the convective Q -value is affected by the change in temperature in the block. Observing the plot and equation, it can be concluded that the convection Q value is directly related to the block temperature linearly; the slope of ~ 114.5 is the factor that relates these values to each other.

The plot shown in Figure 6.8 along with the heat transfer relation in Figure 6.10, used to find a calibration curve to relate the data points. The trends found in these plots can be applied to calculations in future tests with other fluids in the HHFTF.

6.5 Measurement Uncertainty

As mentioned in section 6.4.3, there is a significant amount of heat that is being lost between the block and the channel. To characterize the heat losses within the system, several calculations were performed from the test data. Unifrax 1600 High Temperature Paper with a thickness of 1 mm (0.0394") was used as insulation and was placed between the cradle and test

section to minimize conduction heat transfer between the surfaces. A photo of this assembly can be seen in Figure 6.11.



Figure 6. 11: Test Section and Cradle Assembly with paper insulation.

To define the effectiveness of the insulation, a thermal resistance calculation was performed using the temperatures from the test section and cradle as the boundary conditions. The data found from Test 3 (Section A) was used in the method described in section 6.3.2. A ten second increment from the test was averaged to get the temperature values. To get the temperature of the test section, an average of the six test section temperatures was used. Since the line and chamber are in vacuum during this period, these temperature readings accurately reflected the test section temperature. Eqs. 6.7 and 6.8 were used to find the heat transferred between the surfaces. Figure 6.12 illustrates a simplified image of the resistance network used.

$$R = \frac{L_{thickness}}{k_{insulation} * A_{contact}} \quad (6.7)$$

$$Q = \frac{T_{TS} - T_{cradle}}{R} \quad (6.8)$$

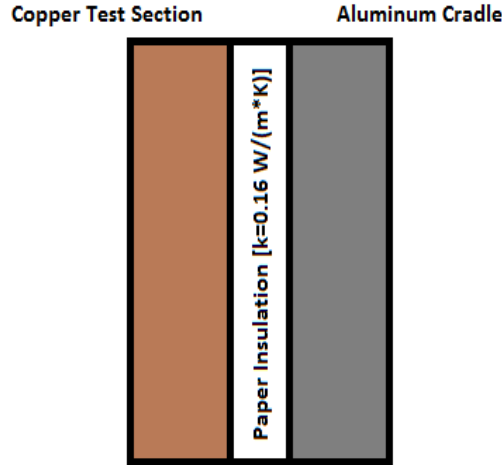


Figure 6. 12: Resistance Network used for analysis.

The heat transferred across this network ranged from 16 to 60 J/s (56 to 200 Btu/hr). The average loss found to be 33.84 J/s (115.57 Btu/hr). Based on the results from Tests 1 through 3, the loss through this interface was less than 2.5% of the total heat of the system. Conclusively, the loss at this interface was clearly present in the data.

The heat loss in the system due to radiation was found using equation Eq. 6.9. The temperature of the block and the vacuum chamber temperature were used as the variables for this analysis.

$$Q_{rad} = \varepsilon * \sigma * A_s * (T_s^4 - T_{surr}^4) \quad (6.9)$$

σ represents the Boltzmann Constant and was taken as $5.670373E-8 \text{ W/(m}^2\text{*K}^4\text{)}$; ε is the emmissivity of polished copper, taken as 0.05. A_s is the surface area of the copper block, at 0.1245m^2 or 193 in^2 . Figure 6.13 shows the trend of radiation increase as the block heats up. The range for this loss was found to be from about 4 to 69 J/s (13.6 to 235 btu/hr).

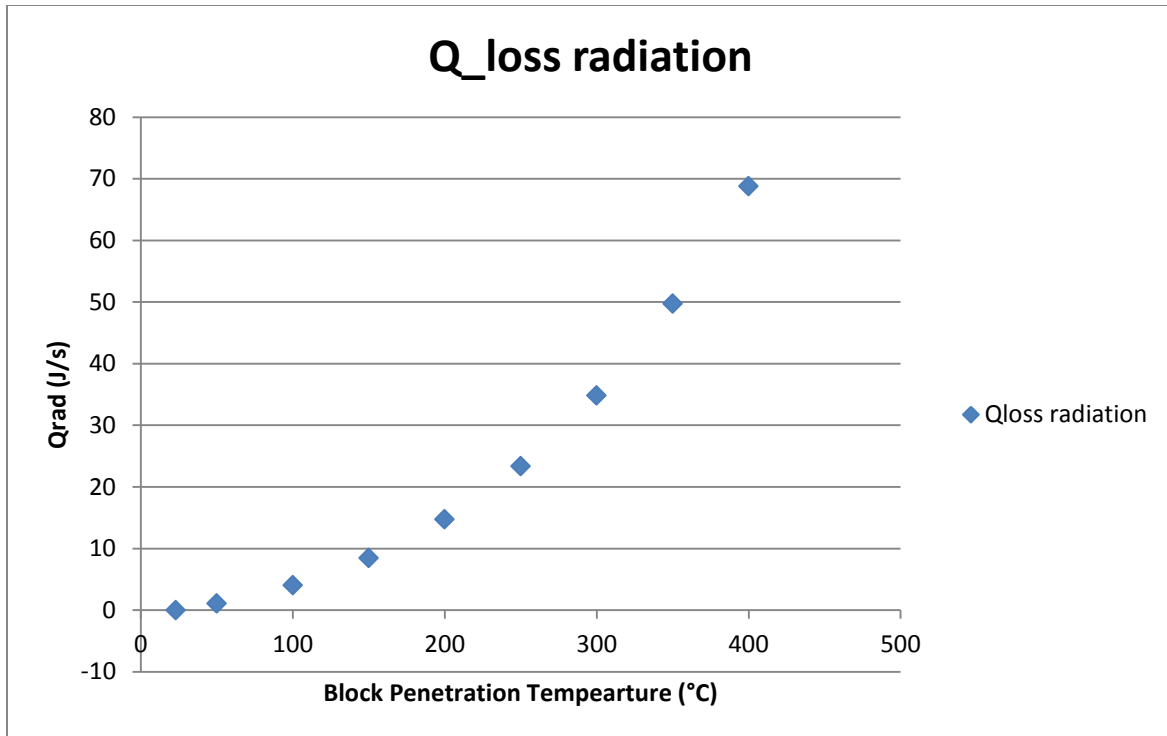


Figure 6. 13: Q_{loss} due to radiation as Block Temperature increases.

Although the losses of the system were found, the difference in heat rate values between the conduction and convection method shows that there is an additional loss in the system. This may be through conduction loss in the stainless steel stand, convection through leaks in the vacuum chamber, additional radiation losses, or heat transferred through walls of the vacuum chamber when the block is heated.

Chapter 7: Conclusion

7.1 Conclusion

The analyses that were performed from the test data serves as a valid representation of the heat transfer model for the HHFTF at the cSETR. The temperature of the block was used as the controlled variable in the experimental test matrix and was monitored via a GUI that was read temperature, pressure and flow rates of the system. A total of three water flow tests were completed. All the tests that were performed supported a general trend and successfully presented valid data.

The data was analyzed using two different heat transfer methods including a convection-based model and a conduction-based model. The comparison of data allowed a correlation to be made between conduction and convection heat flow in the system. Overall, the conduction heat transfer rate was much higher than the convection heat transfer rate, around 3.1 times as high. The losses in the system were calculated to observe the efficiency of the system and concluded that losses were present due to heat conduction and radiation in the HHFTF.

This heat transfer model is transferrable to other experimental setups and defines a solid concept analyzing a heating model.

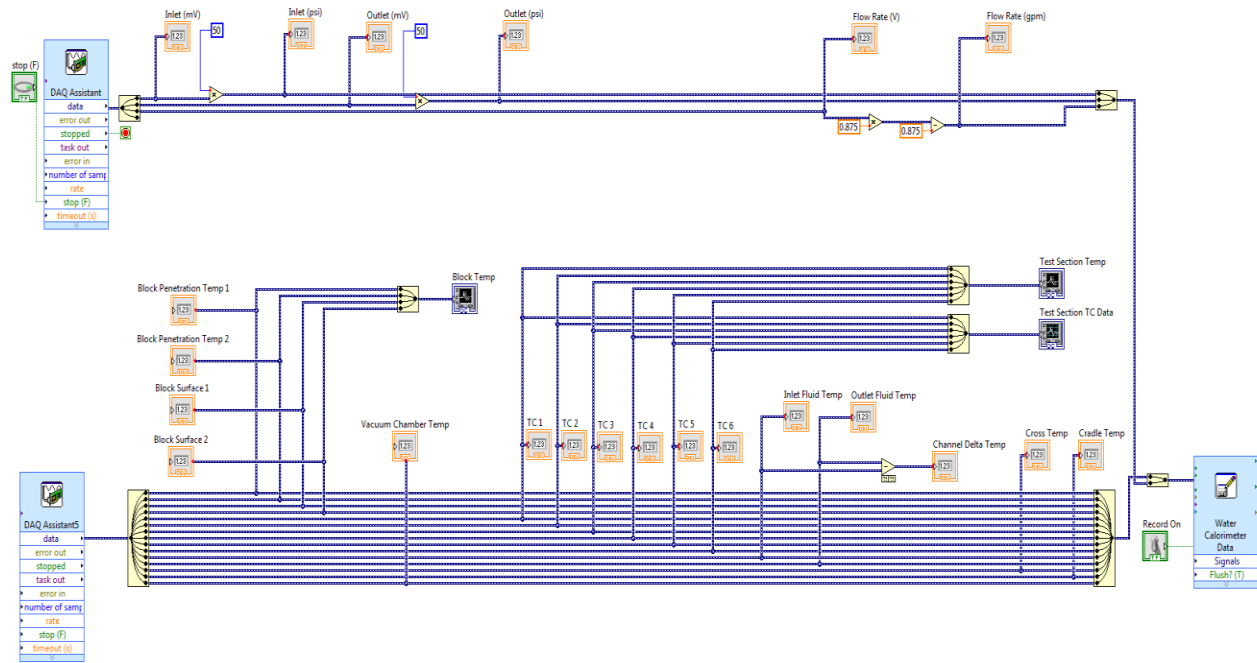
7.2 Future Work

Knowledge of the heat transfer model is essential in truly understanding the conditions that the liquid methane is exposed to and how the methane flow changes with heat flow rate. In the future, the model found in this project can be correlated to future methane tests to accurately analyze the data of the system.

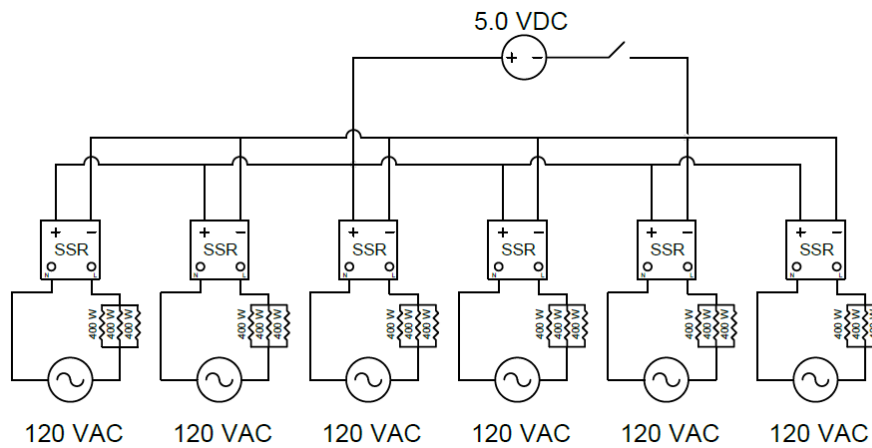
References

- [1] Neill, T. Judd, D. Veith, E. and Rousar, D. 2009. Practical Uses of Liquid Methane in Rocket Engine Applications. *Acta Astronautica*, Vol. 65, pp. 696-705.
- [2] Morehead, R.L. 2011. Project Morpheus Main Engine Development and Preliminary Flight Testing. 47th AIAA Joint Propulsion Conference Atlanta, AIAA 2011-5927, San Diego, CA.
- [3] Duesberg, J. 2012. Rocket TechnologyL: Thrust Chamber.
<http://www.kmakris.gr/RocketTechnology/ThrustChamber>. Boeing Engineering.
- [4] Bates, R. W. Mass, E. D. Irvine, S. A. and Auyeung, T. P. 2004. Design of a High Heat Flux Facility for Thermal Stability Testing of Advanced Hydrocarbon Fuels. Air Force Research Laboratory, F04611-99-C-0025, Edwards AFB, CA.
- [5] Van Noord, J. 2010. A Heat Transfer Investigation of Liquid and Two-Phase Methane. NASA Glenn Research Center, NASA/TM-2010-216918, Cleveland, OH.
- [6] Cook, R.T. 1984. Methane Heat Transfer Investigation. NASA Marshall Space Flight Center, NASA-CR-171199, Huntsville, AL.
- [7] Gage, M. L. and Rosenberg, S. D. 1990. Hydrocarbon Fuel/Combustion-Chamber-Liner Materials Compatibility. NASA Lewis Research Center. NASA CR-185203, Cleveland, OH.
- [8] Mass, E. Irvine S. A. Bates, R. and Auyeung T. 2004. A High Heat Flux Facility Design for Testing of Advanced Hydrocarbon Fuel Thermal Stability. Air Force Research Laboratory, 4847, Edwards AFB, CA.
- [9] Trejo, A. 2014. An Experimental Investigation of the Cooling Channel Geometry Effects on the Internal Forced Convection of Liquid Methane. PhD Dissertation, University of Texas at El Paso, ProQuest/UMI.
- [10] Bergman, T. L., Lavine, A.S., Incropera, F.P, and Dewitt, D.P. Fundamentals of Heat and Mass Transfer, 7th ed. New Jersey: Wiley.
- [11] Cengel, Y. A., and Ghajar, A. J. 2010. Heat and mass transfer: Fundamentals & applications. 4th ed. New York: McGraw Hill.
- [12] Chieh, C. 2008. Calorimetry: Measuring Heats of Reactions. University of Waterloo, CA.

Appendix



A1: Block diagram for the LabVIEW program used.



A:2 Detailed Electrical Schematic for cartridge heaters.

A:3 Detailed instrumentation list.

Item	Make	Model	Range	Accuracy	Use	Quantity
Exposed tip type E thermocouple	Omega Engineering	EMQSS-125E-6	-200 to 900°C(-328 to 1652°F)	1.7°C or 0.5% above 0°C, 1.7°C or 1.0% below 0°C	Test section wall temperature measurement	6
Exposed tip type K thermocouple	Omega Engineering	KMQSS-125E-6	-200 to 1250°C(-328 to 2282°F)	2.2°C or 0.75% above 0°C, 2.2°C or 2.0% Below 0°C	Heating Block temperature measurement	4
Ungrounded type K thermocouple	Omega Engineering	KMQSS-125U-6	-200 to 1250°C(-328 to 2282°F)	2.2°C or 0.75% above 0°C, 2.2°C or 2.0% Below 0°C	Vacuum chamber temperature measurement	1
Ungrounded type E thermocouple	Omega Engineering	EMQSS-125E-6	-200 to 900°C(-328 to 1652°F)	1.7°C or 0.5% above 0°C, 1.7°C or 1.0% below 0°C	Fluid inlet and outlet temperature	2
Exposed type K thermocouple	Omega Engineering	EMQSS-125E-6	-200 to 1250°C(-328 to 2282°F)	2.2°C or 0.75% above 0°C, 2.2°C or 2.0% Below 0°C	Cradle temperature measurement	1
Thin Film Cryogenic Pressure Transducer	Omega Engineering	PX1005L-500AV	0 to 3.45 MPa (0 to 500 psia)	±0.25%	Test section inlet/outlet pressure measurement	2
Thermocouple Input Module DAQ device	National Instruments	NI 9213	Refer manual	Refer manual	Thermocouple data acquisition	2
Terminal Block with SCC Expansion Slots DAQ device	National Instruments	NI SCC-68	Refer manual	Refer manual	Pressure transducer and flow meter data acquisition	1
Pressure transducer process meter and controller	Omega Engineering	DP25B-E-A	0 to 100 mV	±0.02% of reading	Pressure transducer signal conditioning	3
Convection-enhanced Pirani Sensor	Kurt J Lesker	K31714S	1×10^{-3} to 1.0×10^3 Torr (1.9×10^{-5} to 19 psi)	±<1%	Vacuum chamber pressure measurement	1
Digital Convection Pirani Vacuum Gauge Controller	MKS	HPS 947	1.0×10^{-3} to 1.0×10^3 Torr (1.9×10^{-5} to 19 psi)	±<1%	Vacuum chamber pressure digital reading	1

A:4 Detailed Experimental Testing Procedure

High Heat Flux Test Facility (HHFTF) Water Calorimeter Test Procedure

Introduction

The growing interest in deep space exploration has brought the attention to regeneratively-cooled (regen) engine design because of the advantages regenerative cooling presents in comparison to dump cooling or film cooling. Liquid methane (LCH₄) is a low toxicity propellant that is being studied for bipropellant fuel systems. However, one of the challenges with LCH₄ is that there is limited empirical data regarding subcritical methane heat transfer.

To provide empirical cooling data for LCH₄, the High Heat Flux Test Facility (HHFTF) was developed at the center for Space Exploration Technology Research (cSETR) at the University of Texas at El Paso (UTEP). At the cSETR there is an effort in the study of sub-scaled single cooling channel test articles.

The following document presents a water calorimeter test procedure. Particularly, the purpose of the test is to develop a method to calculate the heat flux being transferred to the test article. This is based on channel fluid flow characteristics and the geometric constraints of the high heat flux test facility. The theory behind finding the heat flux through the test section is by using a form of the general heat transfer equation: $Q = \dot{m} * c_p * \Delta T$. The heat being transferred into the fluid inside the test channel, using measured with fluid properties, will be correlated to the heat being introduced from the trapezoidal section of the heat source, the heating block.

****Block temperature and test section geometry are the factors that *vary* in the test matrix.**

Test Matrix Example:

block temperature (°C)	duration (sec)	mass flow rate (kg/s)	TS temperatures (avg)	Q= m*cp*dT	Penetration T1	Penetration T2	Q trapezoid
24 (room)	15						
50	15						
100	15						
150	15						
200	15						
250	15						
300	15						
350	15						
400	15						

Test Setup

High Heat Flux Test Facility (HHFTF)

The HHFTF system focuses on fluid heating by supplying a constant heat flux to a cooling channel test section whose conditions are monitored by temperature and pressure instrumentation. Components incorporated in the HHFTF include a 316 L stainless steel (SS) test stand, a heating block made of C12200 copper, heating cartridges are placed inside the heating block and controlled with a manual switch [connected with solid state relays], a cradle made of 6061-Al, and C18200 copper test sections.

Moreover, the instrumentation used in the HHFTF includes various sensors and transducers; these include vacuum gauge controllers, pirani sensors, pressure transducers, as well as probe thermocouples. The experiment is performed in vacuum to minimize convective losses and prevent oxidation damage to the components. To minimize conduction losses, there is no metal-metal contact between the surfaces within the vacuum chamber by using high temperature ceramic plates and Unifrax1600 paper insulation, which has a temperature stability of 1600°C and a thermal conductivity of $k = 0.16 \text{ W/mK}$ (@ $T_{\text{mean}} = 600^\circ\text{C}$). A detailed list of the instrumentation that is used in the system is found in Appendix (A3).

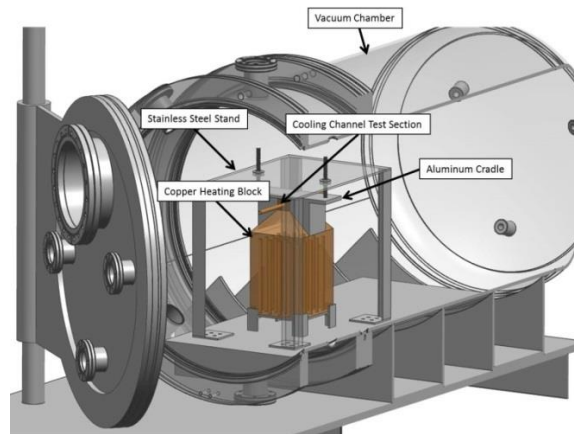


Fig. 1. High heat flux test facility components.

Fluid Schematic

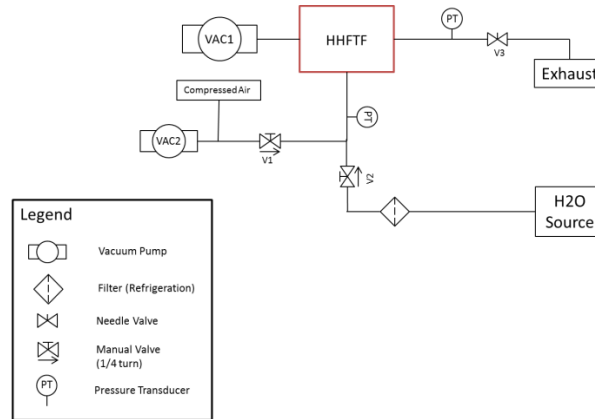


Fig. 2 displays the schematic of the integrated system which includes the HHFTF.

Electrical System Schematic

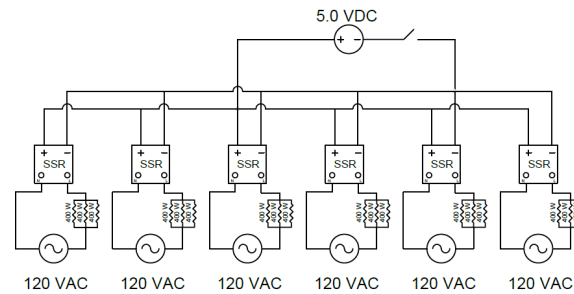


Fig. 3. SSRs and cartridge heaters schematic.

Graphical User Interface (GUI)

The figure below shows a snapshot of the LabVIEW GUI used to monitor the conditions of the HHFTF. More specifically, the GUI displays pressures and temperatures that are being read inside the vacuum chamber, this includes temperatures of the block and test section, the vacuum chamber. Also, the graphs located on the bottom right provide the channel wall temperature profile versus time. The “Record On” switch located on the top right is used to activate data recording; the program will record data when the switch is pointing upwards.

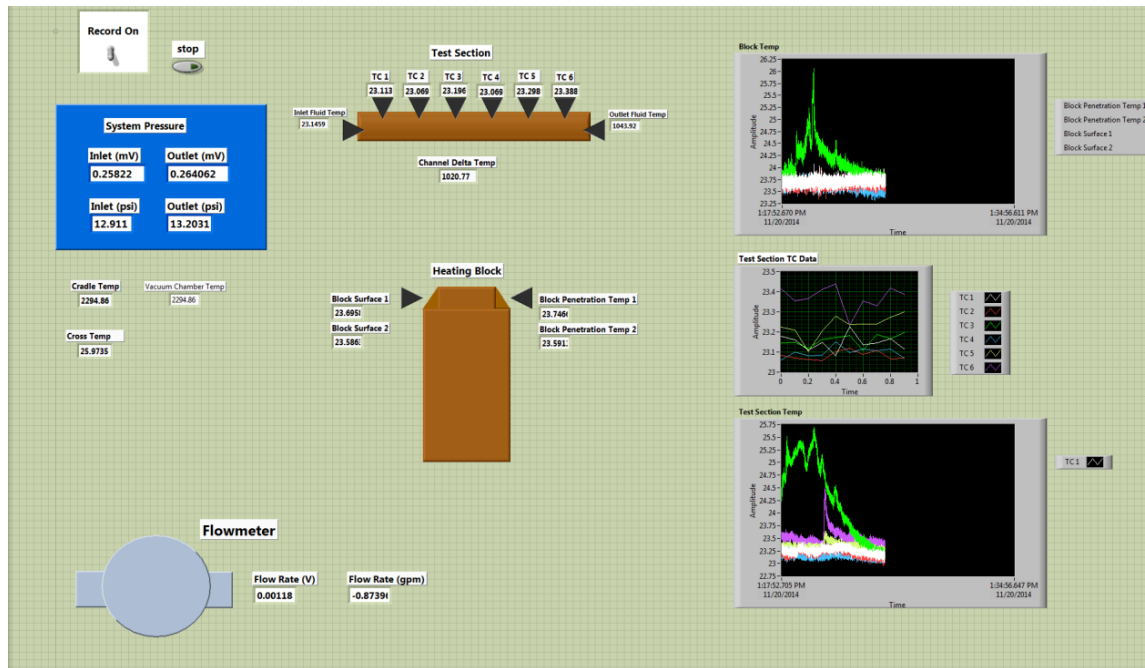


Fig. 2. GUI used during testing.

Procedure

Refer to Appendix A for team role assignments.

Pre-testing procedure:

1. Safety [All team members]
 - a. Put on appropriate lab-required personal protective equipment (PPE).
 - b. Other safety precautions
 - i. Tie long hair
 - ii. Hold back loose clothing
 - iii. Take off loose jewelry
2. HHFTF Preparation [Test Conductor]
 - a. Ensure that all the components are assembled properly inside the vacuum chamber.
 - i. Thermocouples
 - ii. Copper block
 - iii. Heating cartridges
 - iv. Test section
 - v. Cradle

- vi. SS stand
- b. Use a multi-meter to check resistances and electrical continuity within the setup.
 - i. Check that all cartridge heaters work properly by measuring the resistance across each SSR
 - 1. Resistance across each relay per group (3 cartridge heaters) is 12 ± 1 ohms.
 - ii. Ensure all the thermocouples that are contacting a surface are positioned correctly to get accurate readings.
 - 1. Use continuity option on the multi-meter
- c. Close vacuum chamber and secure with bolts.
 - i. Connect VAC1 to the chamber using the available O-ring connection and turn on.
 - ii. Activate the Pirani vacuum gauge controller and monitor vacuum chamber pressure till it reaches desired levels.
 - 1. Chamber vacuum levels: 0.05 ± 0.01 Torr
- 3. Inspection of all instrumentation and equipment. [Test Technician]
 - a. Checklist of water calibration materials
 - i. Water source [available in lab facility]
 - ii. Compressed air [purge gas]
 - iii. High heat flux test facility (HHFTF) [present in cSETR lab]
 - iv. Plastic hosing (Water)
 - 1. 2 parts
 - a. [A] Includes Refrigeration filter attached (inlet)
 - i. Longer hose: from water source to test section inlet
 - b. [B] Shorter hose (outlet)
 - i. Shorter hose: from test section outlet to drain
 - v. Beaker (500 mL)
 - 1. To measure flow rate
 - vi. Timer
 - 1. To measure flow rate
 - b. Ensure all valves and piping is operating properly.

- i. Check all connecting locations for leaking
 1. Open all the (3) valves.
 2. Use the air gun to pressurize the lines.
 3. Apply Snoop Leak Detector fluid at joining localities.
 4. If fluid bubbles, tighten appropriate fittings.
- c. Electrical instrumentation
 - i. Run the LabVIEW program titled “High Heat Flux Test Facility” located in the “LabVIEW programs” folder in the computer’s desktop.
 1. Run the LabVIEW program by using the option in the Front Panel window.
 2. Create a folder in the “Water Calibration Test Data” folder that entails the conditions being tested.
 - a. Ensure that results will be saved in this folder
 - ii. Confirm that all pressure transducers and thermocouples are reading ambient conditions (13 ± 1 psia and $23 \pm 3^{\circ}\text{C}$ respectively).
 1. (1) Inlet PT
 2. (1) Outlet PT
 3. (6) Test Section [TS] Temperatures
 4. (4) Block Temperatures
 5. Other Temperature Readings
 - a. (1) Vacuum Chamber temperature
 - b. (1) Cradle temperature
 - iii. Turn on power supplies and adjust to required voltage.
 1. SSRs: 5 VDC.
 - a. 18 cartridges/6 relays (120 V, 10 amps)
 - iv. Ensure that the electrical power needed for the test setup is ready for use.
 1. US Standard type 3 prong plugs are connected to the standard [NEMA 5–15R] sockets that are provided in the lab (120 V, 10 amps).
 - a. Power is provided to the following devices:
 - i. (6) Power for the solid state relays (SSR) heaters.

- ii. (1) Pirani vacuum gauge controller [vacuum chamber pressure]
 - iii. (2) Power for the vacuum pumps
 - iv. (2) Power for the voltage boxes
- 4. Pre-Testing Preparation [Test Technician and Test Conductor]
 - a. Connect tubing to the experimental setup.
 - i. Tube [A]
 - 1. Connect longer side of the tube to the water source (spigot) located above the setup and tighten the hose clamp with a flathead screwdriver.
 - 2. Connect one end of the filter pump to the water source and the other end to the inlet connection to the test section.
 - ii. Tube [B]
 - 1. Connect the swaged side to the exhaust of the test facility and place the other end to the drain opening on the floor.
 - b. Prepare for data collection.
 - i. Ensure that LabVIEW program outputs the data file into a folder titled “Water Calibration Test Data” on the computer’s desktop.
 - ii. Verify the specifications of the test conditions.
 - 1. Conditions are based on the test matrix.
 - c. Water source
 - i. Open the water valve and exhaust (needle) valve (V2 and V3 respectively).
 - ii. Open the water source by pulling the lever till it reaches a vertical position.
 - 1. This will fill the hose with water.
 - a. Allow water to flow through the test article and into the [B hose] exhaust drain.
- 5. Testing Procedure [Test Conductor]
 - a. Heating the copper block
 - i. Manually activate cartridge heaters by following a 3 sec on/off cycle.

1. Use the manual switch located on the switch panel (red, rightmost switch).
 - ii. Heat the block until desired block temperature is reached (based on test matrix).
 - iii. At the desired block temperature, monitor the test section's skin temperatures till the readings are flat-lined (at steady state).
- b. Data recording and flow rate measurement will be performed *concurrently* and each process is described below.
 - i. Data recording [Test Conductor]
 1. Turn on the record option ('Record On') for the LabVIEW program and record the data for 15 seconds [press 'Record On' again to deactivate data recording].
 - ii. Flow rate measurement [Test technician]
 1. Confirm the test section temperature and block readings are at steady state and take the beaker and the timer to the drain; measure the time it takes to fill the beaker 500 mL with the waste water.
 2. Record this as the volume flow rate for analysis.
 3. Dump the measured water down the drain for disposal.
- c. Repeat steps 5.a and 5.b (above) for each data point on the test matrix.
 - i. During the test, the water is running continuously through the block.
6. Post-testing procedure [Test Technician]
 - a. After the final data point has been recorded, purge the system as described below.
 - i. Close V2 and remove the endcap that is in the compressed air inlet.
 - ii. Place the air gun at the opening and pressurize the line.
 - iii. Open V1 and purge the line with compressed air till the [B] hose is blowing out dry air.
 1. Another team member must hold the [B] hose steady during the purge.
 - b. Disassemble the hose used for the calibration and use the air gun to purge the hose after it has been removed.

- c. Close valves V2 and V3 and turn on VAC2 to pull vacuum in the lines. When the line pressure levels are 2 ± 1 psia, close V1 and turn off VAC2.
 - i. This is to prevent any oxidation from building up inside the line.
- d. Unplug or turn off all electrical sources
 - i. Unplug
 1. Solid state relays
 - ii. Turn off
 1. Voltage sources
- e. Leave the vacuum chamber closed to avoid metal oxidation within the setup. Turn off the (VAC1) vacuum allow the block cool on its own. This may take several hours.

Emergency Procedure

All safety considerations were taken and an emergency procedure was developed in case of an unwanted occurrence. Red lines are shown below to avoid a catastrophic failure of the hardware or facilities.

Red Lines:

- Line pressure must remain less than 350 psia.
- Block temperature must remain less than 500°C.

Risks and Hazards:

Hazard	Risk	Mitigation
Flammability (short)	Electrical Spark or Ignition	Insulation of wires to prevent a short circuit Fire extinguisher

In the event of an emergency:

1. Close water source.
2. Relieve residual system pressure as per “Post-testing procedure.”
3. Inform other teams of the situation; evacuate lab if necessary.

4. Contact Abraham Trujillo at (915) 747-7398.
5. If life/facility is in danger, contact UTEP police at (915) 747-5611.

Appendix A

Current role assignments for testing –Fall 2014

Test Supervisor – Abraham Trujillo

- Oversee the team and ensure the test procedure and matrix are being followed.
- Carry out the emergency procedure.

Test Conductor –Linda Yoon

- Monitor the test via the LabVIEW GUI.
- Heat the copper block.
- Prepare for data collection.

Test Technician – Edgardo Flores

- Inspect instrumentation, equipment, and testing area.
- Open/close valves.

Appendix B

Instrumentation List

Table 1. Detailed instrumentation list.

Item	Make	Model	Range	Accuracy	Use	Quantity
Exposed tip type E thermocouple	Omega Engineering	EMQSS-125E-6	-200 to 900°C(-328 to 1652°F)	1.7°C or 0.5% above 0°C, 1.7°C or 1.0% below 0°C	Test section wall temperature measurement	6
Grounded type E thermocouple (extra)	Omega Engineering	EMQSS-125G-6	-200 to 900°C(-328 to 1652°F)	1.7°C or 0.5% above 0°C, 1.7°C or 1.0% below 0°C	Test section wall temperature measurement	6
Ungrounded type E thermocouple (extra)	Omega Engineering	EMQSS-125U-6	-200 to 900°C(-328 to 1652°F)	1.7°C or 0.5% above 0°C, 1.7°C or 1.0% below 0°C	Test section wall temperature measurement	6
Exposed tip type K thermocouple	Omega Engineering	KMQSS-125E-6	-200 to 1250°C(-328 to 2282°F)	2.2°C or 0.75% above 0°C, 2.2°C or 2.0% Below 0°C	Heating Block temperature measurement	6
Grounded type K thermocouple	Omega Engineering	KMQSS-125G-6	-200 to 1250°C(-328	2.2°C or 0.75% above 0°C,	Heating Block temperature	6

(extra)			to 2282°F)	2.2°C or 2.0% Below 0°C	measurement	
Ungrounded type K thermocouple (extra)	Omega Engineering	EMQSS-125U- 6	-200 to 1250°C(-328 to 2282°F)	2.2°C or 0.75% above 0°C, 2.2°C or 2.0% Below 0°C	Heating Block temperature measurement	6
Ungrounded type K thermocouple	Omega Engineering	EMQSS-125U- 6	-200 to 1250°C(-328 to 2282°F)	2.2°C or 0.75% above 0°C, 2.2°C or 2.0% Below 0°C	Vacuum chamber temperature measurement	1
Ungrounded type K thermocouple	Omega Engineering	EMQSS-125U- 6	-200 to 1250°C(-328 to 2282°F)	2.2°C or 0.75% above 0°C, 2.2°C or 2.0% Below 0°C	Cradle temperature measurement	1
Thin Film Cryogenic Pressure Transducer	Omega Engineering	PX1005L- 500AV	0 to 3.45 MPa (0 to 500 psia)	±0.25%	Test section inlet/outlet pressure measurement	2
Thermocouple Input Module DAQ device	National Instruments	NI 9213	Refer manual	Refer manual	Thermocouple data acquisition	2
Terminal Block with SCC Expansion Slots DAQ device	National Instruments	NI SCC-68	Refer manual	Refer manual	Pressure transducer and flow meter data acquisition	1
Pressure transducer process meter and controller	Omega Engineering	DP25B-E-A	0 to 100 mV	±0.02% of reading	Pressure transducer signal conditioning	3
Convection- enhanced Pirani Sensor	Kurt J Lesker	K31714S	1×10^{-3} to 1.0×10^3 Torr (1.9×10^{-5} to 19 psi)	±<1%	Vacuum chamber pressure measurement	1
Digital Convection Pirani Vacuum Gauge Controller	MKS	HPS 947	1.0×10^{-3} to 1.0×10^3 Torr (1.9×10^{-5} to 19 psi)	±<1%	Vacuum chamber pressure digital reading	1

Vita

Linda Yoon was born in San Diego, California and raised in El Paso, Texas. She attended the University of Texas at El Paso starting in fall of 2008 and graduated with a Bachelor's of Science degree in Mechanical Engineering in December of 2012 and began pursuing her Master's of Science in Mechanical Engineering the following semester. She started working at the Center for Space Exploration Technology Research in the summer of 2012. In the summer of 2013, she started work as a Pathways intern at NASA Glenn Research Center and worked on acoustic analysis, as well as extreme terrain mobility. In the fall of 2014, she accepted an offer from Glenn Research Center and plans to begin her career as an engineer in early 2015.

Permanent Address: 4637 Tumbleweed Ave.

El Paso, TX, 79924

This thesis was typed by Linda Hyemin Yoon.